Prospectus February 2020

Working Title:

Dissolved Organic Matter Dynamics in a Large Temperate River

Laura Logozzo

Committee Members:
Peter Raymond, Chair, Yale University
Tim Eglinton, ETH Zürich
James Saiers, Yale University
Benjamin Twining, Bigelow Laboratory for Ocean Sciences

Abstract

Dissolved organic matter (DOM) is an extremely important variable in aquatic systems: it is a source of carbon, nitrogen, and phosphorous, thus influencing nutrient cycling and aquatic productivity; it limits the amount of UV and visible light in inland waters; its complexation with trace metals can result in their mobilization (or removal) in aquatic systems; and it's a significant part of the global carbon cycle, with the amount of carbon in DOC stored in oceans alone being far greater than the amount of carbon in CO_2 in the atmosphere. Rivers connect the terrestrial landscape with oceans; they are both pipes and reactors, meaning that they both transform and transport material such as DOM. I propose studying DOM dynamics seasonally in a large temperate river, the Connecticut River.

DOM UV-vis measurements have been widely used as a cost-efficient and less time-consuming method of estimating DOM composition. However, the presence of iron in filtered water samples results in overestimations of DOM UV-vis absorption. Despite the development of correction factors for iron, they are rarely applied. In Section 1, I address the implications of failing to correct for iron by examining the impacts of iron on two commonly measured DOM UV-vis parameters, by quantifying the impact of iron at 5 sites along the Connecticut River over a 1.5 year period starting in July 2018 and for 7 smaller tributaries in the Connecticut River watershed in the summer 2019. Sampling and measurements (total Fe, Fe(II), Fe(III), DOC, a_{254} and $SUVA_{254}$) have been completed, and a draft manuscript is provided here (Section 1).

Iron is a limiting nutrient in coastal zones and oceans. Rivers were not thought to be sources of iron to oceans, since >90% of dissolved iron is lost in estuaries due to an increase in salinity. Recently, however, studies have shown that rivers can be significant contributors of iron to coastal zones and open oceans if the iron is complexed with DOM. In Section 2, I propose addressing the role of DOM in iron speciation, concentration, and export by the Connecticut River to the Long Island Sound. Seasonal and downstream variability are particularly important; to address this we have been sampling 5 sites along the Connecticut River bi-weekly for 1.5 years, with a plan to complete a 2 year dataset (sampling ending July 2020). We measure total Fe, Fe(II), Fe(III), DOC, and a range of DOC optical parameters on 2 fraction sizes. Section 2 describes our sampling strategy and methods in more detail, what has been collected thus far, and some preliminary analysis of a portion of our dataset.

Despite being one of the largest carbon reservoirs globally, riverine DOC sources are poorly quantified. Carbon age indicates whether DOC in rivers is sourced from surface soils or deeper sequestered soils. I propose estimating DOC age and flux at one site on Connecticut River seasonally at a high temporal resolution (bi-weekly) using ^{14}C. This will be compared to previous ^{14}C measurements at the same site to look at long-term trends. This will address when in the year older DOC is mobilized in rivers, and whether there is an overall trend towards older DOC. Samples are already being collected and stored for conversion to CO_2 for later analysis. Sampling will end July 2020, and samples will be prepared in August 2019. This research question is funded by the NASA CT Space Grant. Section 3 describes our objectives and research strategy in more detail.

1. The effects of iron on DOM optical measurements in rivers

1.1. Introduction and Significance

Within the last two decades, dissolved organic matter (DOM) optical properties, such as absorption and fluorescence, have been compared to DOM chemical composition markers in order to derive estimates of DOM quality parameters. For example, DOM aromaticity can be approximated using the specific UV absorption at 254 nm, ($SUVA_{254}$), which is the absorption of DOM at 254 nm (a_{254}) divided by the DOC concentration (Weishaar et al. 2003). Hernes and Benner (2003) found the DOM absorption coefficient at 350 nm (a_{350}) to be associated with dissolved lignin concentration. DOM molecular weight can be approximated using the log-transformed absorption slope from 275-295 nm ($S_{275\text{-}295}$) or the slope ratio (S_R), which is the ratio of the slopes at 275-295 nm and 350-400 nm (Helms et al. 2008). Even general groups of compounds and functional groups present in DOM can be estimated using fluorescence excitation-emission matrices (EEMs) combined with PARAFAC analysis (Stedmon et al. 2003). The advancement in these methods and analyses has allowed for a more comprehensive analysis of DOM quality and quantity across a variety of systems, and at higher frequencies, due to the speed and cost-efficiency of the methods.

DOM optical measurements are most commonly performed on 0.2 μm filtrate (and sometimes 0.45 or 0.7 μm filtrate); however, UV-vis absorption in this fraction by other chemical species besides DOM has been acknowledged (Weishaar et al. 2003; Xiao et al. 2013; Poulin et al. 2014). One such species is iron, which can pass through a 0.2 μm filter and also absorbs light in the UV-vis range (Weishaar et al. 2003; Poulin et al. 2014), where DOM absorption occurs and where numerous DOM quality parameters are measured (SUVA, $S_{275\text{-}295}$, $S_{350\text{-}400}$, S_R). Total iron in natural waters is composed of ferric and ferrous iron, Fe(III) and Fe(II), respectively. In general, iron absorption has been attributed to ferric iron, Fe(III), while the absorption of ferrous iron, Fe(II), has been shown to be negligible (Poulin et al. 2014). Fe(III) absorbs differently depending on its speciation (Stefánsson 2007). Furthermore, Fe(III) formed by Fe(II) oxidation was shown to have a different absorption curve compared to inorganic Fe(III) added directly to solution, though this difference was determined to be negligible in the range most often measured for DOM (Poulin et al. 2014).

While some studies have determined that the impacts of Fe(III) on DOM UV-vis absorption for iron concentrations typical of surface waters are negligible (Weishaar et al. 2003), others have shown that Fe(III) absorption in these wavelengths can be significant (Xiao et al. 2013; Poulin et al. 2014). For example, Kritzberg and Ekström (2012) found that increasing iron concentrations and iron absorption was an important factor in the observed "brownification" of northern inland waters, with iron accounting for up to 74% of the change in water color. Xiao et al. (2015) also found that iron accounted for up to 83.2% of riverine water color in Swedish rivers. Xiao et al. (2013) found that Fe(III) bound to DOM accounted for a 1.8 to 2.3-fold increase in absorption at 280 nm depending on the type of DOM; this was even greater for absorption in longer wavelengths, with an up to 5.3-fold increase in absorption at 550 nm.

Fe(III) absorption follows Beer's law, and the increase in absorption linearly increases with increasing iron concentration (Weishaar et al. 2003; Xiao et al. 2013; Poulin et al. 2014). As such, corrections based on Fe(III) concentrations have been developed (Poulin et al. 2014). These corrections only require the Fe(III) concentration. However, while total iron and Fe(III) concentrations can be easily measured, Fe(III) corrections are rarely applied to DOM optical measurements. Thus, reported values of DOM UV-vis absorption are likely overestimated in some systems. In particular, Poulin et al. (2014) suggests likely iron interference in DOM UV-vis measurements in "surface waters that are acidic, collected from peatlands, drain watersheds with iron-rich minerals, or exchange with suboxic, iron(II)-rich waters (e.g., groundwater exchange or lake turnover." In this paper, we discuss the impacts of Fe(III) on DOM absorption at 254 nm and SUVA in the surface waters of the Connecticut River for 5 sites across a 214 km stretch and over ~1.5 years and for 7 sites sampled during the summer 2019. We had the following research objectives:

(1) Quantify the effects of Fe(III) absorption on DOM optical measurements, a_{254} and $SUVA_{254}$, for samples collected from the Connecticut River mainstem and across 7 streams and rivers
(2) Examine seasonal and land use patterns in Fe(III) impacts on DOM UV-vis absorption

1.2. Methods

1.2.1. Sampling Sites

Five sites along a 214 km stretch of the Connecticut River mainstem were sampled every other week from July 2018 to December 2019 and one of the five sites (Thompsonville) every other week since April 2018 (Table 1.1, Figure 1.1a). All sites are actively monitored USGS stream gages with stage, temperature, pH, dissolved oxygen, conductivity, turbidity and fluorescent DOM measured every 15 min, and two out of the five sites are measured every 15 minutes for discharge (Thompsonville and Middle Haddam). As such, these parameters can be compared to our measured samples at the time of collection. In addition to the bi-weekly sampling, 7 sites ranging from headwaters to large rivers throughout the Connecticut River watershed were sampled once during the Summer 2019 (Table 1.2, Figure 1.1b).

Table 1.1. Sites along the Connecticut River mainstem sampled bi-weekly.

Site	Location	USGS ID	Latitude	Longitude	# Samples
NORT	Northfield, MA	01161280	42.68333	–72.47194	32
THOM	Thompsonville, CT	01184000	41.98722	–72.60583	40
HADD	Middle Haddam, CT	01193050	41.54167	–72.55361	31
ESSX	Essex, CT	01194750	41.35148	–72.38437	30
OLYM	Old Lyme, CT	01194796	41.31250	–72.34639	30

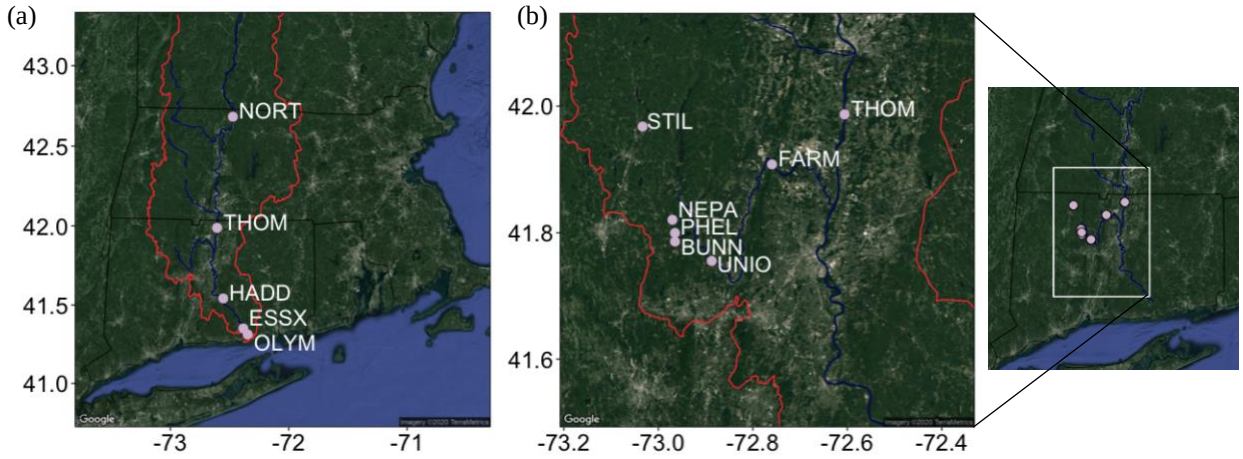

Figure 1.1 (a) Sites along the Connecticut River sampled bi-weekly and (b) sites sampled once during the summer 2019.

Table 1.2. Connecticut River watershed sites sampled once during the Summer 2019.

Site (4-letter code)	USGS ID	Latitude	Longitude	Drainage Area (km^2)	Forest (%)	Wetland (%)	Agriculture (%)	Developed (%)
Bunnell Brook (BUNN)	01188000	41.78621	–72.96483	10.6	60.5	9.6	16.6	11.6
Farmington River at Tariffville, CT (FARM)	0118995	41.90828	–72.75935	1494.0	68.6	7.2	4.6	14.8
Nepaug River (NEPA)	01187800	41.82065	–72.97010	61.6	74.9	6.2	8.9	8.3
Phelps Brook (PHEL)	01187830	41.79978	–72.96488	6.5	65.8	14.8	9.9	8.3
Still River (STIL)	01186500	41.96792	–73.03344	220.2	76.1	7.3	3.4	9.6
Connecticut River Thompsonville, CT (THOM)	01184000	41.98722	–72.60583	25019.3	75.8	5.0	6.2	5.0
Farmington River Unionville, CT (UNIO)	01188090	41.75555	–72.88704	979.0	77.0	7.0	2.9	7.7

1.2.2. Sample Collection and Storage

All sample bottles were acid-soaked with 1N HCl for at least 24 hours, and then rinsed 4 times with Milli-Q water. Samples were collected at each site using an acid-rinsed polypropylene bucket or jug, which was rinsed three times with sample water before collection. Samples were filtered on-site through Sterivex polyethersulfone membrane 0.22 μm filters (Sterivex #SVGP01050) using acid-washed PharMed BPT tubing and a peristaltic pump. 0.22 μm filters and tubing were purged with at least 250 mL of milli-Q water, and then with at least 50 mL of sample. For Fe(II) collection for the Connecticut River mainstem bi-weekly sampling, an acid-washed

Tygon E-3603 tube was attached to the outlet of 0.22 μm filter, and the tube placed in the bottom of an acid-washed 60 mL amber bottle. The bottle was then over-filled 3 times with the 0.22 μm filtrate, the tube slowly removed, and the bottle capped immediately, ensuring that no air bubbles were trapped inside the sample bottle. This was placed immediately on ice, and then at 4°C in the lab until analysis. For the summer 2019 sampling event, Fe(II) measurements were performed directly in the field (See Section 1.2.4) immediately after sampling and 0.22 μm filtering. For total dissolved/soluble iron and DOM, two 120 mL HDPE bottles were filled with filtrate from the 0.22 μm filter. Both samples were immediately placed on ice in the field and then at 4°C in the lab until subsequent filtration and analysis. Starting in the summer of 2019, unfiltered samples to measure total unfiltered iron were collected at the CT River mainstem sites in 30 mL acid-soaked HDPE bottles, and frozen immediately.

1.2.3. 0.02 μm filtration of CT River mainstem samples

Half (about 30 mL for ferrous iron and 120 mL for total iron/DOM) of the 0.22 μm sample was sequentially filtered through a Whatman Anopore inorganic membrane (Anodisc) 0.02 μm filter (Whatman # 89203-116). All filtering equipment (e.g., vacuum flask) was acid-soaked in 1 N HCl, rinsed 4 times with milli-Q water, and then baked at 450°C for 5 hours. Sequential filtration of a portion of the 0.2 um filtrate using the 0.02 μm filter was conducted on the Connecticut River mainstem samples within 4 days of collection. The 0.02 μm filter were placed on the vacuum filtration setup and rinsed with at least 300 mL of milli-Q water, and then with at least 10 mL of sample. Roughly 30 mL of the 0.2 μm Fe(II) filtrate was then 0.02 μm filtered, and Fe(II) was immediately measured on both size fractions (See Section 1.2.4). One of the two HDPE bottles containing 0.2 μm filtrate was then filtered through the 0.02 μm filter on the same vacuum setup, and transferred to a clean 120 mL HDPE bottle. The 7 sites sampled as part of the summer 2019 sampling event were not 0.02 μm filtered.

1.2.4. Measurements

Fe(II) was measured using the 1,10-phenanthroline method on the Hach DR900 or the Hach FerroVer Pocket Colorimeter II within 4 days of collection and immediately after 0.02 μm filtration, for the Connecticut River mainstem sites. Samples were stored at 4°C until measurement. Total iron concentrations were measured using the Hach FerroVer method on the Hach DR900 or the Hach FerroVer Pocket Colorimeter II within 1 month of collection, and stored at 4°C until measurement. Standards were prepared before each run according to the Hach FerroVer method sheet (DOC 316.53.01458) for total iron and 1,10-phenathroline method sheet (DOC 316.53.01049) for ferrous iron. Fe(III) concentrations were calculated by subtracting the measured Fe(II) concentrations from the total Fe concentrations.

Dissolved organic carbon (DOC) concentrations were measured as non-purgeable organic carbon (NPOC) on a Shimadzu TOC-V Analyzer within 1 month of collection, and stored at 4°C before measurement. Standards and quality checks were measured for each run and were prepared according to Shimadzu protocol.

Dissolved organic matter UV-vis measurements were performed on a Horiba Aqualog fluorometer, within 2 weeks of collection. Decadal absorption coefficients were performed with a 1 cm pathlength at 3 nm wavelength intervals. S_R was calculated using the log-transformed absorption slopes from 275 – 295 nm ($S_{275-295}$) and 350 – 400 nm ($S_{350-400}$). The specific UV absorbance at 254 nm ($SUVA_{254}$) was calculated by dividing the decadic a_{254} by the DOC concentration, according to Weishaar et al. (2003).

For all measurements, differences between the 0.22 and 0.02 μm fraction sizes were calculated by difference.

1.2.5. 1.2.5. Fe(III) corrections to UV-vis measurements

Corrections due to Fe(III) interference in UV-vis measurements were applied to a_{254} values, using a correction factor of 0.0653 for decadic absorption at 254 nm and the Fe(III) concentration, as proposed by Poulin et al. (2014). The Fe(II) fraction was assumed to have a negligible impact on UV-vis absorption (Poulin et al. 2014).

1.2.6. 1.2.6. Calculations

$SUVA_{254}$ was calculated by dividing the measured a_{254} by the DOC concentration. Fe(III)-corrected $SUVA_{254}$ was calculated by dividing the corrected a_{254} by the DOC concentration, and the percent overestimation in $SUVA_{254}$ was calculated by dividing the difference in uncorrected and corrected $SUVA_{254}$ by the corrected $SUVA_{254}$. We also quantified the impacts of Fe(III) on UV-vis absorption in our system by comparing the difference in absorption between the 0.22 μm and 0.02 μm fractions and differences in Fe(III) and DOC (See Results). Post-correction, only the bulk (<0.22 μm) fractions were used in analysis for the sake of consistency, as this is the fraction most commonly used for DOM analyses.

1.3. Results

1.3.1. Differences in fraction sizes

We examined the impacts of Fe(III) on DOM optical properties by comparing the 0.22 μm and 0.02 μm size fractions for the CT mainstem sites. DOC concentrations <0.22 μm ranged from 2.05 to 6.48 mg/L, with an average concentration of 3.31 mg/L. This was very similar for the 0.02 μm filtrate, which had an average DOC concentration of 3.22 mg/L (Table 1.3). Total Fe ranged from 0.002 to 0.255 mg/L in the <0.22 μm fraction, with an average of 0.087 mg/L, and from 0 to 0.110 mg/L, with an average of 0.018 mg/L, in the <0.02 μm fraction. Fe(II) ranged from 0 to 0.067 mg/L in the <0.22 μm fraction (average of 0.020 mg/L) and from 0 to 0.044 mg/L (average of 0.011 mg/L) in the <0.02 μm fraction. Fe(III) ranged from 0 to 0.212 mg/L (average of 0.020 mg/L) in the <0.22 μm fraction, and from 0 to 0.044 mg/L (average of 0.011 mg/L) in the <0.02 μm fraction. The average a_{254} in the <0.22 μm fraction was 11.7 m^{-1}, ranging from 5.9 to 28.0 m^{-1}. For the <0.02 μm fraction, the average a_{254} was 10.4 m^{-1}, ranging from 5.2 to 25.2 m^{-1} (Table 1.3). The difference in DOC between the 0.22 and 0.02 μm fractions was not significant ($P = 0.36$), but the difference was significant for total Fe, Fe(II), Fe(III), and a_{254} ($P < 0.01$). Both a_{254} and

$SUVA_{254}$ were significantly greater in the <0.22 fraction the 0.02 µm size fraction ($P < 0.01$). On average, a_{254} in the 0.22 and 0.02 µm fractions was 11.7 and 10.4, respectively (Table 1.3). $SUVA_{254}$ in the 0.22 and 0.02 µm fractions was 3.50 and 3.19, respectively (Table 1.3).

The difference in DOC between the 0.22 µm and 0.02 µm fractions was less than 4.2%, demonstrating that the majority of the DOM present in the 0.22 µm fraction is also present in the 0.02 µm fraction. Conversely, 81.4% of the Fe(III) was removed from the 0.22 µm fraction with 0.02 µm filtration (Figure 1.2). Similarly, the difference in Fe and Fe(II) between the two fractions was, on average, 81.9% and 48.9%, respectively (Figure 1.2), and this difference was significant ($P < 0.01$). The difference in a_{254} between the two fractions was 12.3%, which was 3 times greater than the difference in DOC. The difference between the two fractions for a_{254} ranged from 0.086% up to 28.9% (Table 1.3). Additionally, the difference in $SUVA_{254}$ between the two fractions was, on average, 10.2%, which is also more than two times the difference in DOC between the two fractions. The difference in $SUVA_{254}$ between the two fractions ranged from 0.45 to 27.9% (Table 1.3).

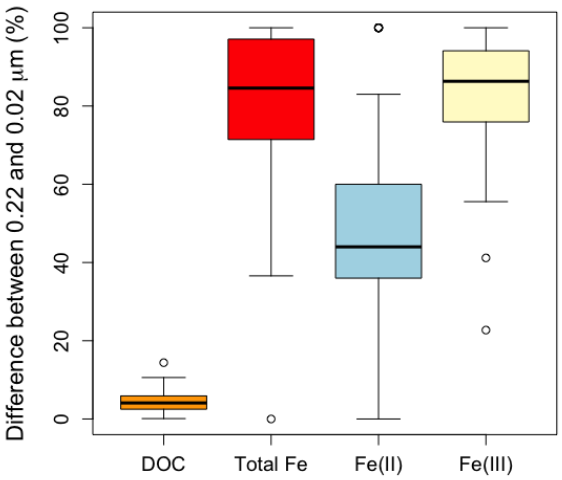

Figure 1.2. Difference in concentration between the 0.22 and 0.02 um fractions for DOC, Total Fe, Fe(II), and Fe(III).

Table 1.3. Average concentrations for DOC, total Fe, Fe(II), and Fe(III), and a_{254} and $SUVA_{254}$ for each size fraction (0.22 and 0.02) and the absolute and percent difference between the size fractions. Ranges listed in parentheses.

	< 0.22	< 0.02	0.22–0.02*	0.22–0.02 (%)*
DOC (mg/L)	3.30 (2.05 to 6.48)	3.22 (2.08 to 6.74)	0.13 (0.004 to 0.41)	4.2 (0.1 to 14.4)
Total Fe (mg/L)	0.087 (0.002 to 0.255)	0.017 (0 to 0.110)	0.070 (0 to 0.193)	81.9 (0 to 100)
Fe(II) (mg/L)	0.020 (0 to 0.067)	0.011 (0 to 0.044)	0.009 (0 to 0.028)	48.9 (0 to 100)
Fe(III) (mg/L)	0.068 (0 to 0.212)	0.012 (0 to 0.067)	0.061 (0 to 0.183)	81.0 (0 to 100)
a_{254} (m^{-1})	11.7 (5.9 to 28.0)	10.4 (5.2 to 25.2)	1.50 (0.007 to 9.7)	12.1 (0.086 to 28.9)
$SUVA_{254}$ (L $mg^{-1}m^{-1}$)	3.50 (2.07 to 5.16)	3.19 (2.11 to 5.16)	0.37 (0.013 to 0.93)	10.2 (0.45 to 27.9)

* Calculated by difference

1.3.2. Fe(III) interference in UV-vis absorption

Comparing DOC concentrations between the 0.22 and 0.02 µm fractions resulted in a strong positive relationship falling approximately on the 1:1 line (Figure 1.3a), demonstrating that there are no appreciable nor systematic differences in DOC concentration between each fraction, as was also indicated by the small average percent difference in concentration (Figure 1.2, Table 1.3). However, despite no difference in DOC concentration, a_{254} and $SUVA_{254}$ were both greater in the 0.22 µm size fraction compared to the 0.02 µm fraction, and the relationship between the two fractions deviated from the 1:1 line (Figure 1.3b-c). While there was no relationship in the

difference in a_{254} and the difference in DOC between the 0.22 and 0.02 µm fractions (Figure 1.4a), there was a significant positive relationship between the difference in a_{254} between the two fractions and the amount of Fe(III) removed during filtration (Figure 1.4b).

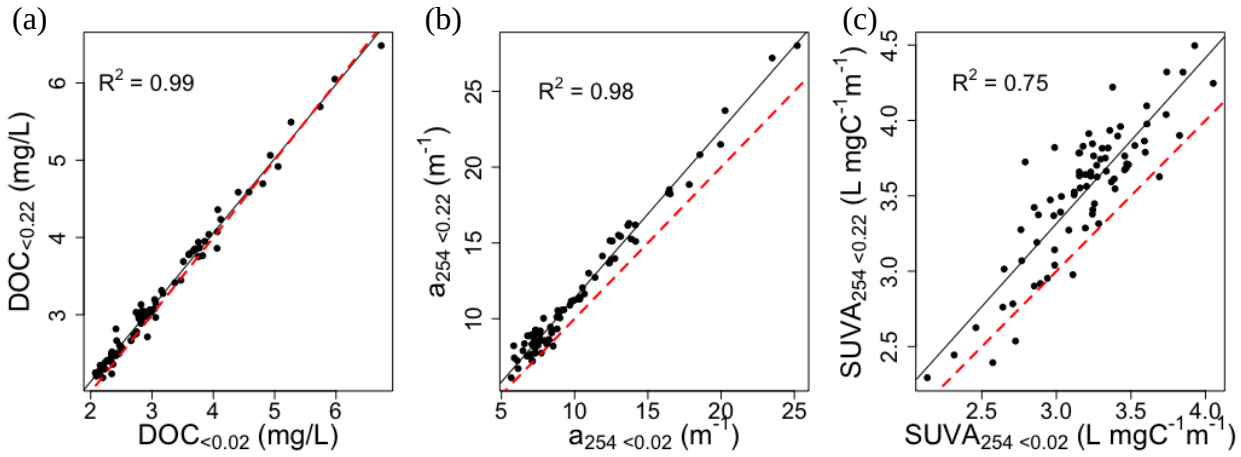

Figure 1.3. Difference between 0.22 µm and 0.2 µm fractions for (a) DOC (b) a_{254} and (c) $SUVA_{254}$. The red dashed line represents the 1:1 line.

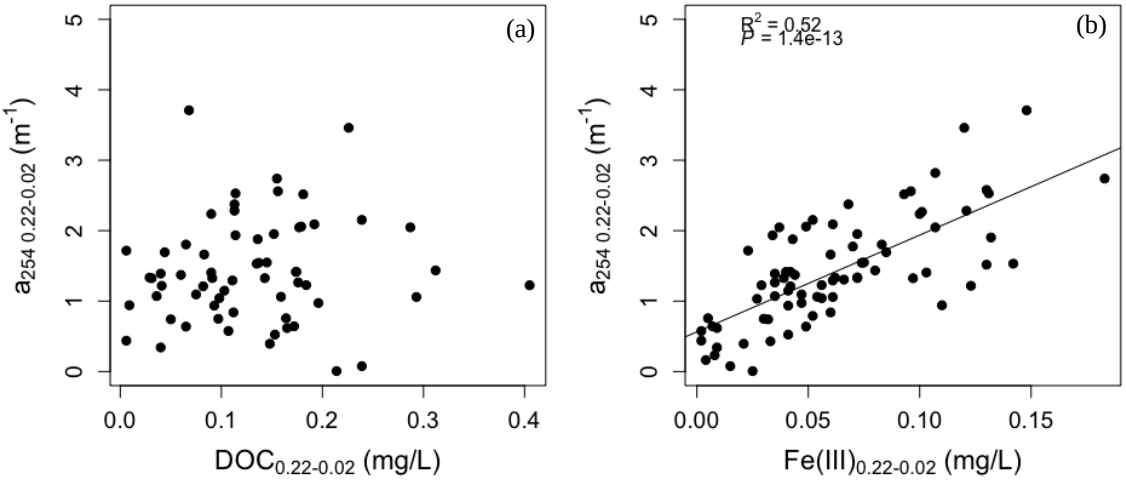

Figure 1.4. Difference in a_{254} between the 0.2 and 0.02 µm fractions (i.e., a_{254} removed by filtration) compared to the difference in (a) DOC concentration and (b) Fe(III) between the 0.2 and 0.02 µm fractions (i.e., DOC and Fe(III) removed by filtration).

1.3.3. Corrections for Fe(III) UV-vis interference

We calculated Fe(III) correction coefficients for a_{254} using the difference in Fe(III) and DOC between the difference in 0.22 and 0.02 µm and <0.02 µm fractions. a_{254} in the <0.22 µm fraction was compared against $Fe(III)_{0.22\text{-}0.02}$, $Fe(III)_{<0.02}$, $DOC_{0.22\text{-}0.02}$, and $DOC_{<0.02}$ using multiple linear regression (Equation 1). The multiple linear regression had an R_2 of 0.95 ($P < 0.01$), and each individual factor (i.e., both DOC and Fe(III) fraction sizes), were significant ($P < 0.01$). Furthermore, the two DOC size fractions (< 0.02 µm and DOC removed by 0.02 µm filtration), had very similar coefficients (4.01 compared to 3.98). The two coefficients for $Fe(III)_{0.22\text{-}0.02}$ and

$Fe(III)_{<0.02}$ were used as Fe(III) correction coefficients; these corrections account for the absorption of potentially two different pools of Fe(III). In order to derive these coefficients, we assume that the only source of UV-vis absorption <0.22 μm is either DOC or Fe(III), as is also done in Kritzberg and Ekström (2012). This resulted in two Fe(III) coefficients, depending on the Fe(III) size fraction: 15.94 for Fe(III) removed by 0.02 μm filtration and 48.48 for Fe(III) smaller than 0.02 μm.

Equation 1. Multiple linear regression used to determine the impacts of Fe(III) <0.02 μm and Fe(III) removed by filtration through 0.02 μm on the a_{254}. R_2 = 0.95 and P < 0.01.

$$a_{254,measured} = 4.01DOC_{0.02-0.22} + 3.98DOC_{<0.02} + 15.94Fe^{3+}_{0.02-0.22} + 48.48Fe^{3+}_{<0.02} - 2.92$$

Applying the Fe(III) correction to a_{254} using the correction coefficient from Poulin et al. (2014), resulted in the relationship between a_{254} and $SUVA_{254}$ in the 0.22 and 0.02 μm fractions falling closer to the 1:1 line (Figure 1.5a and c); however, our correction resulted in the regression between the two fractions falling closer to the 1:1 line (Figure 1.5b and d). Furthermore, while the Poulin et al. (2014) correction improved the fit for $SUVA_{254}$ between the two fractions (uncorrected: R_2 = 0.75, corrected: R_2 = 0.78) (Figure 1.3c and Figure 1.5c), our correction improved the fit even more (R_2 = 0.89, Figure 1.5d). Using either correction, there was no longer any significant difference between a_{254} in the two fractions ($P > 0.1$). The correction coefficients derived in this study results in a 2.44 to 7.4 times greater degree of correction than proposed in Poulin et al. (2014) and similar values from other studies (Weishaar et al. 2003). For the remainder of this analysis, the Poulin et al. (2014) correction coefficient was used rather than the one derived in this study, as a conservative estimate of the potential overestimation of a_{254} and $SUVA_{254}$ due to Fe(III) interference in UV-vis spectra.

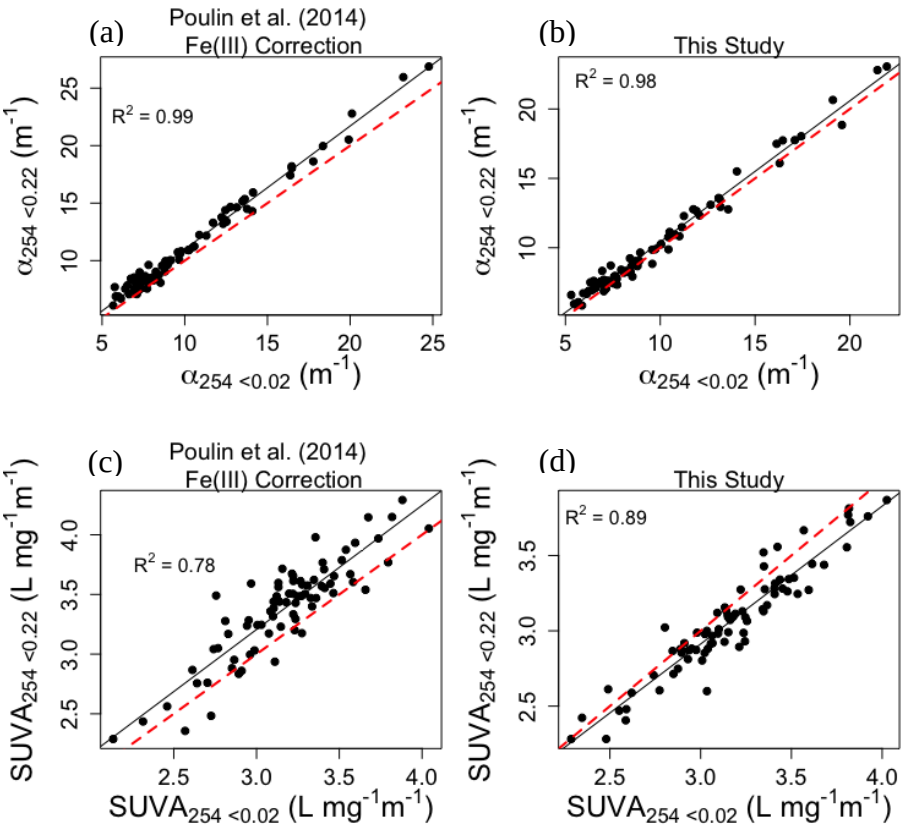

Figure 1.5. Corrected (a-b) a_{254} and (c-d) $SUVA_{254}$ using the (a,c) Poulin et al. (2014) correction and (b,d) the correction factor developed in this study.

1.3.4. a_{254} and $SUVA_{254}$ overestimation

Using the Poulin et al. (2014) correction coefficient, the average percent Fe(III) correction in a_{254} and $SUVA_{254}$ for the CT mainstem sites was 4.0%, with the highest correction being 10.1%. This 10.1% correction led to the overestimation of a_{254} as 15.2 m^{-1} compared to the corrected value of 13.8 m^{-1}, and 3.93 vs. 3.57 L mg^{-1} m^{-1} for $SUVA_{254}$. This correction was for an Fe(III) concentration of 0.212 mg/L. For the 7 smaller watersheds sampled during the Summer 2019, however, the overestimation of $SUVA_{254}$ was overall much greater and with a larger range. The average percent overestimation of $SUVA_{254}$ was 17.7%, with the greatest overestimation being 55.0%. In this case, $SUVA_{254}$ was overestimated as 5.84 compared to 3.77 L mg^{-1} m^{-1}, for an Fe(III) concentration of 0.35 mg/L.

The percent difference in Fe(III) concentration between the 0.22 and 0.02 µm fractions is not necessarily proportional to the percent overestimation of a_{254} or $SUVA_{254}$; for Fe(III) concentrations that were 39.4% different between the 0.22 and 0.02 µm fractions (0.212 and 0.35 mg/L), the percent overestimation of $SUVA_{254}$ was 44.9% different. The best predictor of percent $SUVA_{254}$ overestimation was not total Fe nor Fe(III) concentration, but the ratio of Fe:DOC and Fe(III):DOC (Figure 1.6, R_2 = 0.96 and 0.98, respectively). The slope of the line between the percent overestimation of $SUVA_{254}$ and the Fe(III):DOC ratio was 177.83, which means for every

increase of 0.1 in the Fe(III):DOC ratio, there was an a_{254} or $SUVA_{254}$ overestimation of 17.78%. The average Fe(III):DOC ratio for the Connecticut River mainstem sites was 0.02 whereas for the 7 Summer 2019 sites it was 0.09. The greatest Fe(III):DOC ratio, 0.32 ($SUVA_{254}$ overestimation of 55.0%), occurred at Bunnel Brook and the lowest, 0.00075 ($SUVA_{254}$ overestimation of 0.21%), occurred at Old Lyme in September 2019. Of the 7 summer 2019 sites, the lowest Fe(III):DOC ratio was at the Connecticut River mainstem at Thompsonville (0.015, $SUVA_{254}$ overestimation of 3.46%).

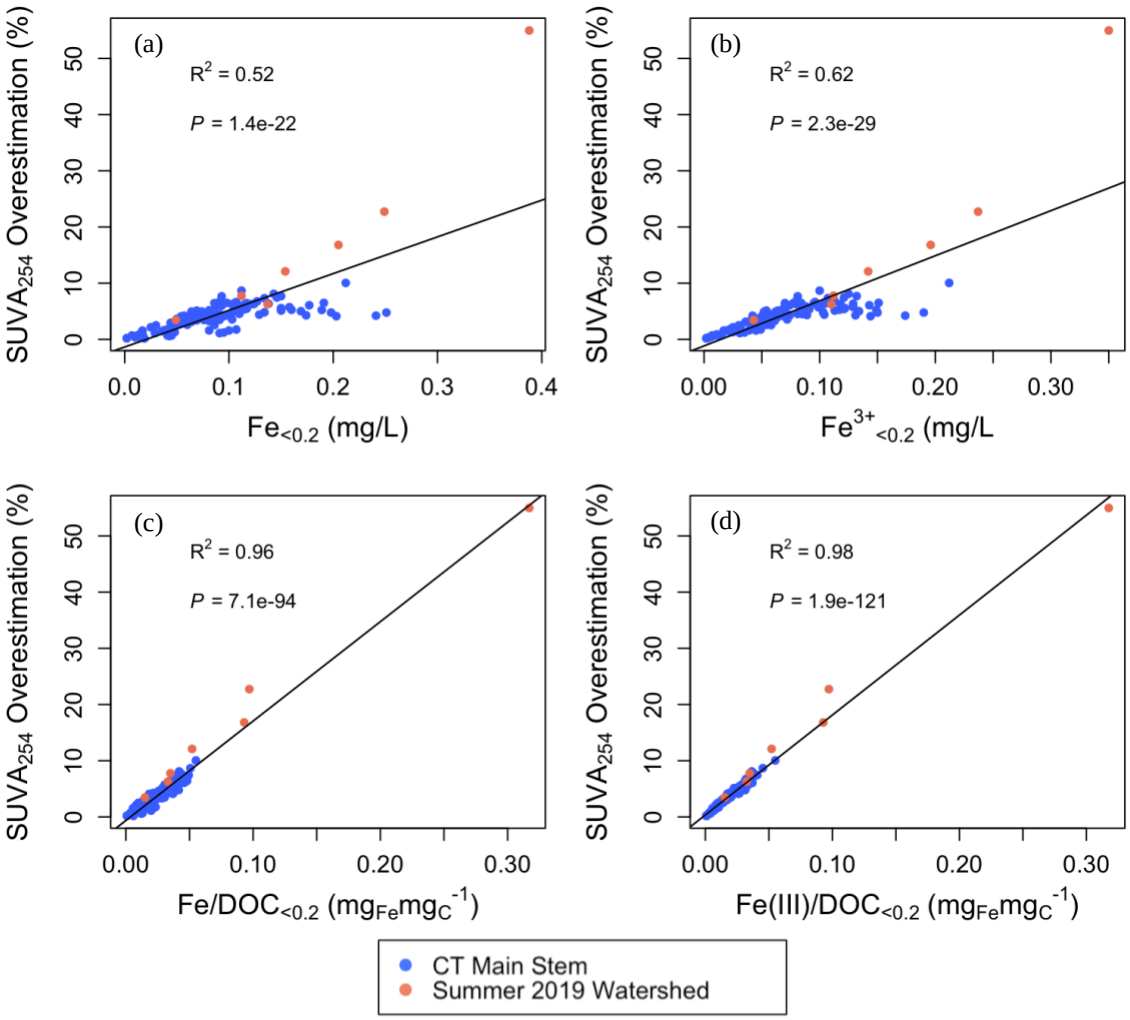

Figure 1.6. $SUVA_{254}$ overestimation compared to (a) total Fe, (b) Fe(III), (c) Fe:DOC, and (d) Fe(III):DOC.

1.3.5. Seasonal patterns in Fe(III) UV-vis interference

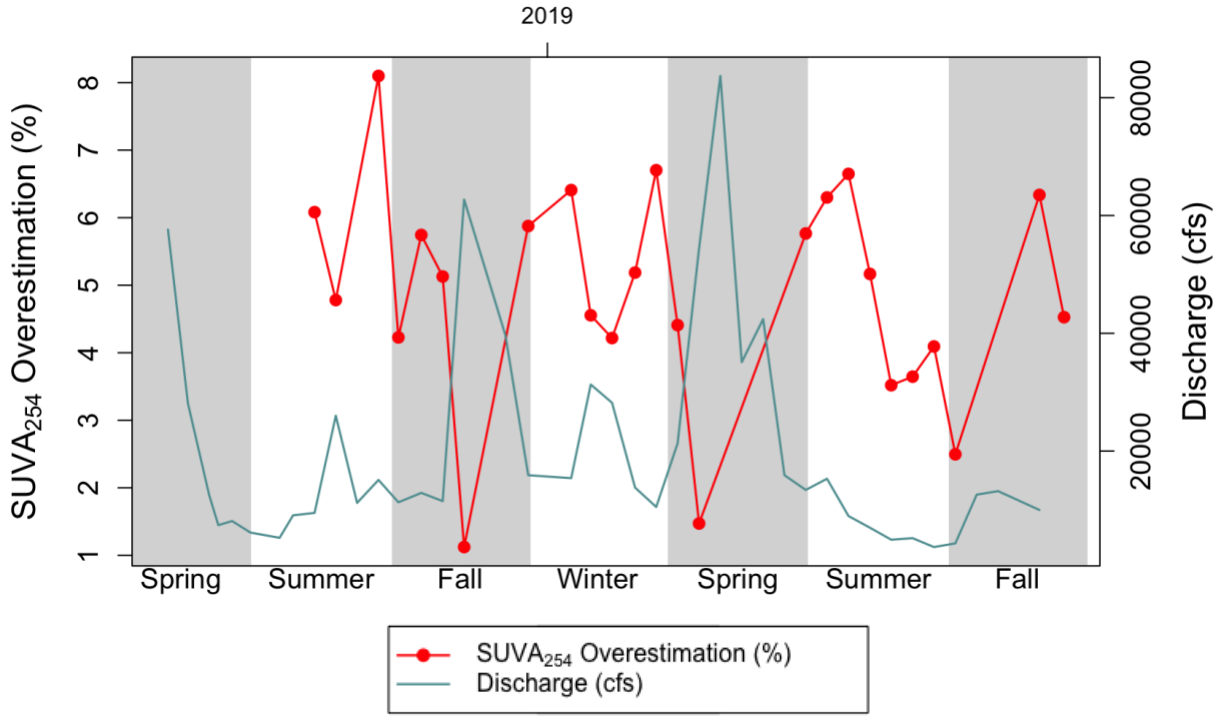

Figure 1.7. Percent overestimation of $SUVA_{254}$ (red circles) and the discharge (blue line) at the Connecticut River mainstem at Thompsonville, CT from 2018 to 2019.

Seasonally, winter had a significantly greater $SUVA_{254}$ overestimation than the summer and fall (P = 0.022 and 0.028, respectively). This was because even though Fe(III) concentrations showed no significant differences seasonally (P > 0.1), DOC concentrations were significantly lower in the winter than all three seasons (P < 0.05), resulting in a higher Fe(III):DOC ratio in the winter. Two high flow events in the Fall of 2018 and Spring in 2019 resulted in extremely low Fe(III):DOC ratios (0.0068 and 0.0067, respectively), and in these cases, the $SUVA_{254}$ overestimation was < 2% (Figure 1.7).

In the Connecticut River mainstem sites Middle Haddam and Thompsonville, we observed a significant, but weak, negative trend between the ratio of Fe(III):DOC and the discharge (R_2 = 0.13, P < 0.01), and therefore, between the percent overestimation of $SUVA_{254}$ and discharge (R_2 = 0.16, P < 0.01). This negative trend was stronger in the winter (R_2 = 0.53, P = 0.015) and spring (R_2 = 0.82, P < 0.01) (Figure 1.8a-b). The relationship in Fe(III):DOC and discharge in the winter and spring was mainly the result of the negative correlation between the Fe(III) concentration and discharge (R_2 = 0.44 and R_2 = 0.77, respectively, P < 0.05, Figure 1.8e-f), with only a weak positive correlation between DOC and discharge in the winter (R_2 = 0.16, P = 0.16, Figure 1.8i) and none in the spring (Figure 1.8j). Conversely, in the summer, there was a positive correlation both between Fe(III) and discharge (R_2 = 0.51, P < 0.01, Figure 1.8g) and DOC and discharge (R_2 = 0.48, P < 0.01, Figure 1.8ik), which overall results in little change to Fe(III):DOC in the summer with discharge (Figure 1.8c). There were no apparent trends in the Fall for Fe(III):DOC, Fe(III), or DOC (Figure 1.8d,j,l).

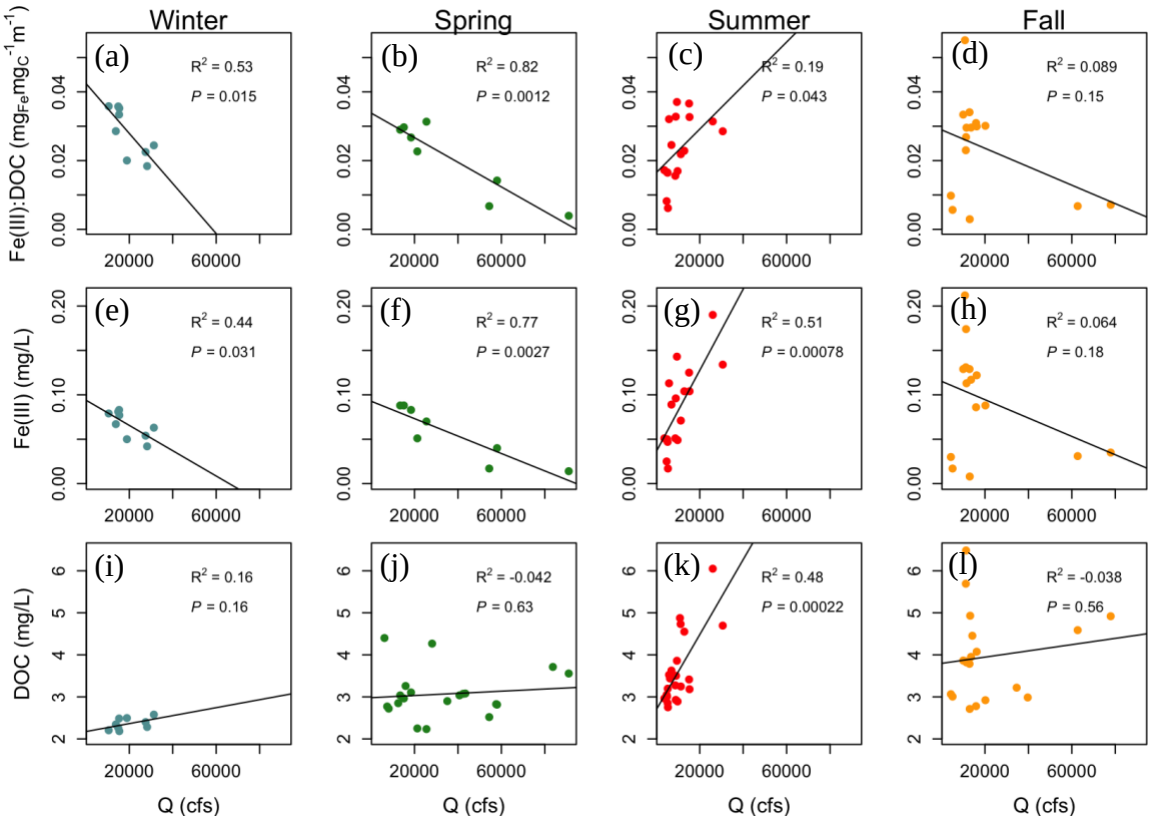

Figure 1.8. Trends in (a-d) Fe(III):DOC, (e-h) Fe(III), and (i-l) DOC compared to discharge (Q) for the winter (blue), spring (green), summer (red), and fall (orange).

1.3.6. Land use and Fe(III) UV-vis interference

For the 7 sites sampled during the Summer 2019, there was a strong positive relationship between the Fe(III):DOC ratio and the percent land cover as agriculture (R_2 = 0.83, P < 0.01). This was the combined result of the strong positive relationship between Fe(III) concentration and percent agricultural land (R_2 = 0.72, P < 0.01), and the strong negative relationship between DOC concentration and percent agricultural land (R_2 = 0.95, P < 0.01). Subsequently, sites with a higher agricultural land cover percentage also had a greater overestimation of $SUVA_{254}$ due to a higher contribution of Fe(III) to UV-vis absorption (R_2 = 0.82, P < 0.01). The opposite trend was observed for forested land cover, with decreasing Fe(III):DOC (R_2 = 0.61, P = 0.023) and $SUVA_{254}$ overestimation (R_2 = 0.057, P = 0.030) with increasing forest cover. This was the result of a decrease in Fe(III) with an increase in percent forest cover (R_2 = 0.051, P = 0.044) and an increase in DOC concentration with higher forest coverage (R_2 = 0.076, P < 0.01). There were no other trends in land cover (e.g., wetland or developed).

Before correcting for $SUVA_{254}$, there were strong relationships between $SUVA_{254}$ and the percent forest and percent agriculture (Figure 1.9a and c, R_2 = 0.65 and 0.75, respectively), and a weak correlation between $SUVA_{254}$ and percent wetland (Figure 1.9b, R_2 = 0.16). However, post-Fe(III)-correction of $SUVA_{254}$, the relationship with percent forest and percent agriculture decreases to R_2 < 0.4 for both, and the relationship with wetlands increases from R_2 = 0.16 to 0.46. Furthermore, multiple linear regression of $SUVA_{254}$ and percent land cover of all four types

resulted in the model showing the greatest weight applied to percent agriculture *before* Fe(III) correction, but for wetlands *post*-Fe(III)-correction.

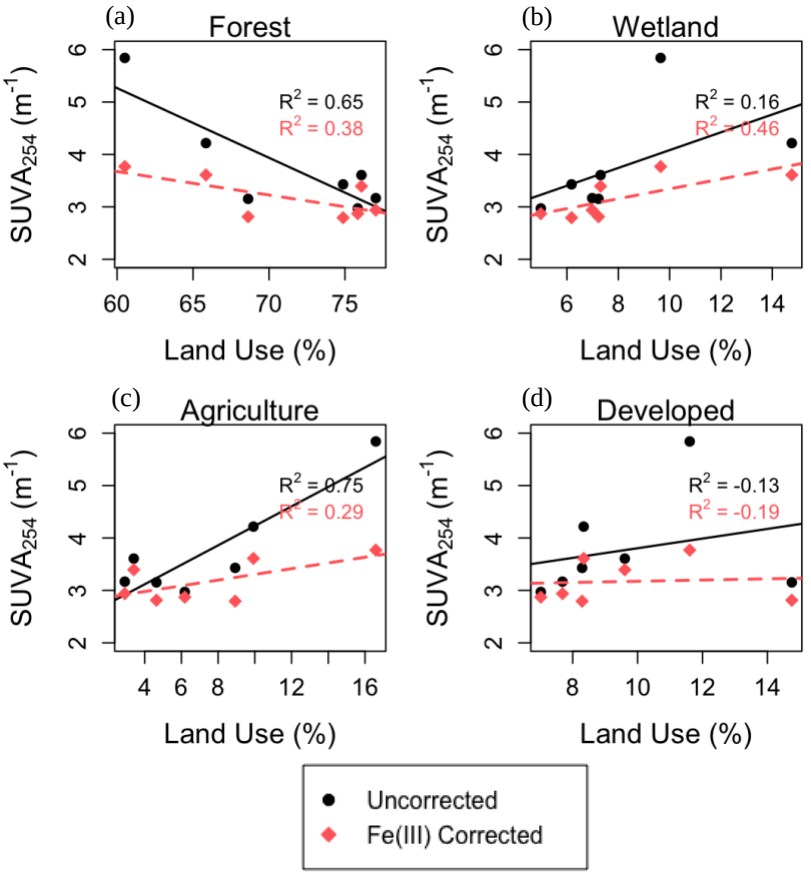

Figure 1.9. Measured and Fe(III)-corrected $SUVA_{254}$ compared to percent (a) forest, (b) weltand, (c) agriculture, and (d) developed land use in the watershed for the 7 sites sampled in the summer 2019.

1.4. Discussion

The greater a_{254} in the 0.22 µm fraction compared to the 0.02 µm fraction suggests that Fe(III) in the 0.22 µm fraction is absorbing in the UV-vis wavelengths, and that when the majority of Fe(III) is removed through 0.02 µm filtration, the absorption is more representative of the DOM pool alone (Figure 1.3 and Figure 1.5). It is therefore apparent that there is an overestimation of a_{254}, which is commonly measured on the <0.22 µm fraction, and that this overestimation is likely due to iron interference. This is supported by the greater amount of scatter in the relationship between $SUVA_{254}$ in the 0.22 and 0.02 µm size fractions before Fe(III)-correction (R_2 = 0.75) compared to after Fe(III)-correction (R_2 = 0.78 and 0.89, respectively, for the Poulin et al. (2014) correction and the correction derived in this study) (Figure 1.3 and Figure 1.5).

The effects of Fe(III) on UV-vis absorption is consistent with past findings (Weishaar et al. 2003; Xiao et al. 2013; Poulin et al. 2014), with increasing Fe(III) concentrations resulting in a linear increase in absorption at 254 nm (Figure 1.4b). By applying the Fe(III) correction factor proposed by Poulin et al. (2014), we found that the overestimation of a_{254} and $SUVA_{254}$, caused by

Fe(III) UV-vis interference, on the Connecticut River mainstem ranged from 0.18 to 10.1%, with an average of 4.0%. This is relatively low. However, we saw overestimations up to 55.0% in smaller streams, and the lowest overestimations occurred in the Connecticut River mainstem sites. This indicates that $SUVA_{254}$ overestimation on the Connecticut River mainstem is likely low compared to other rivers, particularly smaller streams. Furthermore, our study showed a much greater contribution of Fe(III) to a_{254} than is accounted for by the Poulin et al. (2014) correction coefficient and other studies (Weishaar et al. 2003), by a factor of 2.44 for the fraction of Fe(III) removed by 0.02 μm filtration and 7.4 for the <0.02 μm Fe(III) fraction. This could be due to the different absorption spectra for different species of Fe(III) or Fe(III) produced by Fe(II) oxidation (Stefánsson 2007; Poulin et al. 2014), which was not taken into account in the Poulin et al. (2014) correction. Fe(III) smaller than 0.02 μm is likely representative of the organically-bound ferric iron pool (Stolpe et al. 2012; Joung and Shiller 2016), which could have a larger effect on absorption than inorganic Fe(III) colloids or aqueous Fe(III). Given that the Poulin et al. (2014) correction coefficient was used for the Fe(III) corrections in this study, it's likely that the a_{254} and $SUVA_{254}$ overestimation values calculated here are conservative, and that the actual overestimation due to Fe(III) interference is much higher. For example, using our two correction coefficients for the two different pools of Fe(III), the average overestimation of $SUVA_{254}$ due to Fe(III) interference for the Connecticut River sites was 15.4% compared to the average of 4.0% using the Poulin et al. (2014) correction.

The impact of Fe(III) on a_{254} and $SUVA_{254}$ was dependent not only on the concentration of Fe(III), but more importantly, on the ratio of Fe(III) to DOC, which is consistent with past findings (Xiao et al. 2015). When the proportion of Fe(III) to DOC is greater, there was a greater percent overestimation of a_{254} and $SUVA_{254}$. As such, a_{254} and $SUVA_{254}$ overestimation can be significant even when Fe(III) concentrations are not high, if DOC is low. This suggests the potential for a systematic overestimation of a_{254} and $SUVA_{254}$ during periods where the Fe(III):DOC ratio is high. In our system, the Fe(III):DOC ratio, and therefore $SUVA_{254}$ overestimation, was negatively correlated to discharge in the spring and winter. Therefore, at low discharge in these seasons $SUVA_{254}$ is likely overestimated. Given that at low flow there is a lower contribution of aromatic DOM (Hosen et al., *in review*), overestimating $SUVA_{254}$ at low flow would reduce the overall seasonal signal (i.e., increase low $SUVA_{254}$). The smallest overestimation of a_{254} and $SUVA_{254}$ occurred at the Connecticut River mainstem at Old Lyme, which is the most downstream endmember with the highest salinity (average salinity during the time of sampling was 15.0 PSU). It's likely that Fe removal by salinity-induced aggregation relative to lower rates of DOM removal results in a lower Fe(III):DOC ratio, and therefore, a lower overestimation of $SUVA_{254}$. At high salinity, a_{254} and $SUVA_{254}$ overestimation due to Fe(III) interference is likely minimal.

The different relationships between Fe(III) concentration and discharge is well-supported in the literature, with some reporting negative correlations and others reporting positive correlations (Vuori 1995). This is likely due to the complexity of factors influencing riverine Fe concentrations, such as source (Ingri et al. 2006; Stolpe et al. 2012), redox conditions (Shiller 1997; Neal et al. 2008; Ekström et al. 2016), and DOM quantity and quality (Krachler et al. 2005).

In particular, the source of iron plays an important role in dictating the relationship between Fe(III) concentration and discharge; for example, both Stolpe et al. (2012) and Ingri et al. (2006) showed that two dominant types of Fe in boreal river systems, Fe(III)-oxyhydroxides and Fe complexed to DOM (Fe-C), varied with river discharge. Ingri et al. (2006) showed that Fe(III)-oxyhydroxides dominated during low discharge, when Fe(II) entering rivers from groundwater is oxidized to form Fe(III)-oxyhydroxides. Conversely, Fe bound to DOM originating in upper soil horizons was shown to dominate during high discharge events (e.g., storm flows). In the winter in our system, it's likely that the predominant Fe(III) source is groundwater, since DOC concentrations are lower than the other seasons, but Fe(III) is not significantly different, indicating the two are not coupled (i.e., derived from the same source). Furthermore, Fe(III) concentrations in winter decreased with increasing discharge, suggesting dilution of groundwater. Conversely, in the summer when Fe(III) and DOC were coupled and both increase with increasing discharge, the predominant source is likely the terrestrial landscape, either as Fe bound to DOM or mineral Fe from soils. In this case, discharge does not strongly drive Fe(III):DOC ratios, nor $SUVA_{254}$ overestimation, since a discharge-driven increase in Fe(III) results in an increase to DOC as well. This suggests that when Fe-C or Fe from mineral soils is the dominant source of Fe in a river system relative to groundwater, the Fe(III):DOC ratio (and $SUVA_{254}$ overestimation) would not be highly impacted by changes in discharge; a switch from an Fe-C dominated iron pool to an Fe(III)-oxyhydroxide dominated iron pool, however, would ultimately result in an increase in the Fe(III):DOC ratio, and therefore, an increase in a_{254} and $SUVA_{254}$ overestimation. This is likely what occurred in the Connecticut River mainstem in the winter. Therefore, it is the proportion of Fe(III)-oxyhydroxide relative to the total iron pool, rather than just the amount of Fe(III), that ultimately controls the Fe(III):DOC ratio and a_{254} and $SUVA_{254}$ overestimation in the Connecticut River mainstem, seasonally.

There was also a systematic overestimation of $SUVA_{254}$ based on land use. Sites with a higher percentage of agricultural land and a lower percentage of forested land in their watersheds had higher Fe(III):DOC ratios, and therefore, greater percent overestimations of a_{254} and $SUVA_{254}$. This has two potential causes. Firstly, it's possible that higher rates of erosion in croplands of agricultural mineral-rich soil results a greater amount of Fe(III) entering rivers relative to DOC, as was reported in other studies (Xiao et al. 2015). Alternatively, agricultural fields might be preferentially located on more iron-rich soils. The negative correlation with forested soils is caused by an increase in DOC and decrease in Fe(III) concentrations with an increase in the percent forest, and could be the result of more DOM entering rivers from leaf litter, soil organic matter, or directly from vegetation. Furthermore, there is likely less soil erosion in forests compared to agriculture due to stabilization by plants, thus reducing iron loads. Because there is a systematic overestimation in a_{254} and $SUVA_{254}$ based on land use, artifacts of this overestimation were observed when comparing relationships between $SUVA_{254}$ and land use. Trends between $SUVA_{254}$ and the percent agricultural land and percent forested land were stronger before Fe(III)-correction, but post-correction, percent wetland coverage was considered the most important land use factor in predicting $SUVA_{254}$. Therefore, by failing to correct for Fe(III) interference in UV-vis

absorption, observed trends in DOM aromaticity and land use may actually be dominated by relationships between Fe(III):DOC ratios and land use, rather than being truly representative of trends in DOM quality.

In summary, we showed that Fe(III) corrections of DOM UV-vis absorption parameters such as a_{254} and $SUVA_{254}$ are essential in riverine samples, particularly in smaller streams where the percent overestimation, conservatively, can be as high as 50%. We found that different sources or species of Fe(III) may absorb differently; this is currently not accounted for in published Fe(III) correction factors for UV-vis absorption parameters. We found that Fe(III):DOC was the best predictor of $SUVA_{254}$ overestimation, consistent with other studies, which suggests that even if Fe(III) concentrations are low, if DOC concentrations are also low, then the overestimation of $SUVA_{254}$ can still be significant. We also demonstrated a systematic overestimation in these parameters by season and discharge, depending on the source of Fe(III) and its relationship to DOM. Land use played an important role in Fe(III) UV-vis interference, as streams with a higher percentage of agricultural land making up their watersheds had a greater amount of a_{254} and $SUVA_{254}$ overestimation, likely due to greater rates of erosion of agricultural soils rich in minerals such as iron, and lower DOC loads. Not correcting for Fe(III) UV-vis interference showed clear artifacts in trends between DOM aromaticity and land use.

2. The coupled cycling of iron and DOM in the Connecticut River

2.1. Introduction and Significance

2.1.1. Riverine iron export to coastal zones

Iron is an extremely important micronutrient in aquatic ecosystems. Although iron is the third most abundant element on earth, it has an extremely low solubility. This results in low concentrations in aqueous environments. It's estimated that about half the ocean is limited by iron (Abadie et al. 2017) and iron has been suggested as a driving force of nitrogen fixation in the tropics (Tagliabue et al. 2017). Even though iron concentrations in coastal zones are higher than the open ocean, phytoplankton in coastal zones often require more iron (Sunda and Huntsman 1995), and thus coastal zones can still be iron limited (Hutchins and Bruland 1998). While dissolved iron concentrations in rivers and inland waters are relatively high (720 nmol/L, globally (Chester 1990; de Baar and de Jong 2001)), an increase in salinity in estuaries results in salinity-induced iron flocculation, and the majority of dissolved iron is lost before reaching the coastal ocean (Boyle et al. 1977; Sholkovitz et al. 1978; Dai and Martin 1995). As such, it was believed that rivers contribute little dissolved iron to coastal zones and marine environments (1.5×10^9 mol/yr (Dai and Martin 1995; de Baar and de Jong 2001)), and thus rivers are generally not included as sources in ocean biogeochemical models (Tagliabue et al. 2016). Recently, however, the insignificance of rivers in the ocean iron cycle has been disputed (Krachler et al. 2010, 2016; Jirsa et al. 2013; Rijkenberg et al. 2014; Herzog et al. 2020; Vieira et al. 2020), mainly due to the role of dissolved organic matter (DOM) in iron speciation. Numerous studies have shown that a fraction of dissolved iron that is complexed with DOM can escape the estuarine mixing zone (Powell and Wilson-Finelli 2003; Krachler et al. 2005; Rijkenberg et al. 2006; Yang et al. 2017; Herzog et al. 2020), and that the iron bound to DOM is both stable (Rose and Waite 2003) and bioavailable (Krachler et al. 2016, 2019), thus making it a potentially important source in iron-limited regions. However, the size of this fraction is dependent on a variety of factors, such as river discharge (Powell and Wilson-Finelli 2003; Ho et al. 2019; Herzog et al. 2020) and DOM source and composition (Krachler et al. 2005, 2016).

2.1.2. Iron speciation and complexation with DOM

The speciation of iron in aquatic ecosystems is highly variable and is dependent on numerous environmental characteristics, such as redox and light conditions, pH (Neubauer et al. 2013), and DOM quality and quantity. In rivers with a pH between 6.5 and 7.5, soluble ferrous iron, Fe(II), is quickly oxidized to insoluble Fe(III) oxyhydroxides (Vuori 1995), which are present as precipitates, often smaller than 0.45 μm (Buffle et al. 1988). These Fe(III) oxyhydroxides are then removed from rivers through settling on the riverbed, where they can be resuspended depending on stream conditions. Furthermore, Fe(II) is more bioavailable than Fe(III) oxyhydroxides. DOM has been shown to complex with Fe(II), thereby retarding its oxidation and keeping it in its soluble state (Theis and Singer 1974; Koenings and Hooper 1976; Gledhill and

van den Berg 1994; Rose and Waite 2003). Furthermore, Fe(III) can also form complexes or bind with DOM (Shapiro 1964, 1977), which can also reduce iron aggregation (Baalousha et al. 2008). Fe(III) bound to DOM can then be photo-reduced to the more soluble Fe(II) (Francko and Heath 1982; Fujii et al. 2011). Fe(III) hydroxide, another common form of iron, is soluble; however, the solubility of organically-complexed iron is higher, resulting in potentially much higher dissolved iron concentrations when in the organically-complexed form (Powell and Wilson-Finelli 2003). Therefore, DOM binding to iron in aquatic systems generally increases both its solubility and bioavailability compared to other common species of iron such as Fe(III) (oxy)hydroxide, and thus DOM is a driving factor in both iron concentration and iron uptake. Iron-DOM complexes have been documented extensively in freshwater (Vuori 1995; Imai et al. 1999; Nagai et al. 2004, 2006; Hassler et al. 2009; Herzog et al. 2020), coastal zones (Powell and Wilson-Finelli 2003; Rose and Waite 2003; Krachler et al. 2005; Herzog et al. 2020), and seawater (Gledhill and van den Berg 1994).

2.1.3. DOM quality and iron complexation

DOM is a complex mixture of organic compounds, operationally defined as passing through a 0.2 μm filter. In rivers, DOM originates either from the surrounding terrestrial landscape (i.e., leaching from soils or plant matter), in which case it is termed "allochthonous," or from in situ production by algae or microbes, in which it is termed "autochthonous." In rivers, DOM can be consumed, degraded, or transformed by photochemical or microbial degradation. DOM composition is directly related both to its source and to its in-stream transformation, and can be categorized based on groups of compounds that are present. In general, DOM can be divided into three broad groups: humic-like, fulvic-like, and protein-like. Humic-like DOM is made up of compounds such as lignin, tannins, polyphenols, and melanins; it generally has a high molecular weight and high aromaticity. Fulvic-like DOM generally has a lower molecular weight than humic-like DOM, is more soluble and more biologically reactive. Protein-like DOM is composed of amino acids and peptides. In general, allochthonous DOM has a greater contribution of humic-like DOM compared to autochthonous DOM, which is generally associated with protein-like or lower molecular weight humic-like or fulvic-like DOM. Photochemical degradation of DOM has been shown to decrease its molecular weight (Helms et al. 2013b), and microbial degradation has been shown to preferentially remove low molecular weight, protein-like DOM, leaving the overall DOM signal with a higher molecular weight and a more humic-like signal (Medeiros et al. 2017).

DOM complexation with iron occurs predominantly at carboxylic and phenolic sites (Benedetti et al. 1995; Bryan et al. 2002; Xiao et al. 2013). While it is thought to be the humic-like and fulvic-like fractions of DOM that are responsible for metal binding (Vuori 1995; Imai et al. 1999; Nagai et al. 2004, 2006; Krachler et al. 2005; Baalousha et al. 2006; Yang et al. 2017), the heterogeneous and poorly categorized nature of DOM means that the specific organic ligands involved in these interactions are unknown (Benedetti et al. 1995; Kinniburgh et al. 1999). Regardless, DOM source (Nagai et al. 2004; Krachler et al. 2016), aromaticity (Baken et al. 2011; Fujii et al. 2014; Kikuchi et al. 2017), and molecular size (Wu et al. 2004; Hassler et al. 2009; Jirsa et al. 2013; Wang et al. 2017) have all been shown to be important factors influencing iron (or

metal) complexation. Therefore, controls on DOM source, composition, and quality are also expected to control iron concentrations in rivers and, subsequently, iron export to coastal zones.

2.2. Research Objectives

The proposed project would evaluate iron-DOM interactions along a 214 km stretch of the Connecticut River, to quantify the environmental controls, seasonality, and variability of iron and DOM along the aquatic-marine continuum. This would provide a more complete understanding of the controls on riverine iron concentrations and export to coastal zones. Currently, how the transformation and transport of DOM along a downstream riverine gradient affects iron-DOM complexation, iron concentration, and iron export to coastal zones, has been largely unexplored. While the seasonal variability of iron has been examined (Shiller 1997; Joung and Shiller 2016), it is usually examined separately from the seasonal variability of DOM, despite the two being coupled. Thus, the mechanisms behind riverine iron seasonality and variability are difficult to determine directly. Furthermore, most estimates of iron export to coastal zones (de Baar and de Jong 2001) are based off of summer measurements (Dai and Martin 1995), when iron concentrations are sometimes lower compared to other seasons (Shiller 1997; Joung and Shiller 2016); in fact, preliminary results from our study have shown the fall to have a 4 times greater truly dissolved iron concentration at our estuarine endmember than the summer (*data not shown*). Therefore, the significance of rivers to coastal and open ocean iron cycling might be understated, as recent studies have begun to show (Herzog et al. 2020; Vieira et al. 2020). The project has three main research objectives (ROs), described below.

(RO 1): Determine the concentration and proportions of DOM and iron in two size classes in a large temperate river, using 0.22 and 0.02 μm filters

Dissolved iron and DOM are operationally defined as compounds that pass through a 0.2 μm filter. Within the 0.2 um bulk dissolved fraction there are a variety of components of different sizes (Tagliabue et al. 2017; Figure 2.1). Some studies will also separate the dissolved fraction into colloidal and soluble/truly dissolved iron, using filtration through 0.02 μm (Joung and Shiller 2016; Ho et al. 2019), though this is not commonly performed. Other studies use flow field-flow fractionation or ultrafiltration to separate colloidal and soluble pools (Krachler et al. 2005, 2010; Stolpe et al. 2005, 2010, 2012). Separating iron and DOM into soluble/small colloidal and large colloidal pools can provide more detailed information on the types of iron and DOM present, compared to using the commonly measured bulk dissolved fraction alone. Furthermore, the size fractions of iron have been shown to have different sources (Stolpe et al. 2012) and are affected by different riverine processes; therefore, separating the two fractions is essential.

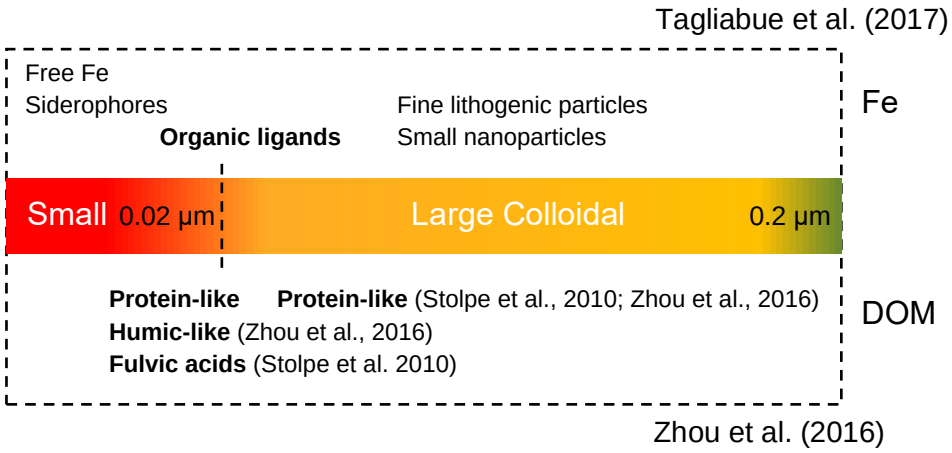

Figure 2.1. Iron and DOM species in the bulk dissolved (<0.2 µm) pool, further divided into the soluble/small colloidal (<0.02 µm) and large colloidal (0.02 to 0.2 µm) pools using discrete cut-offs. Bolded are iron and DOM components particularly relevant to this study. Figure adapted from Tagliabue et al. (2017).

Although some studies have found no correlation between the size fraction of DOM and the size fraction of iron (Koenings and Hooper 1976; Pokrovsky and Schott 2002), many others have shown certain size fractions of DOM to be extremely important for metal complexation (Wu et al. 2004; Hassler et al. 2009; Stolpe et al. 2012; Jirsa et al. 2013; Wang et al. 2017). Jirsa et al. (2013) found that in a creek draining a peat-bog, a "larger" humic-like DOM size class was closely associated with iron and that this larger fraction played a more important role in iron complexation than the "smaller" humic-like fraction. It is important to note, however, that the overall size range in the study was 1 to 10 nm, which represents a relatively small colloidal region (<0.02 µm). Therefore, what is considered "large" in Jirsa et al. (2013) is considered small in others. Stolpe et al. (2012) found extremely small DOM colloids (<8 nm) to be associated with iron. Wu et al. (2004) found that iron was associated with large molecular sized DOM; however, they attributed this larger molecular size to the "bridging," or aggregation, of DOM by metals with high binding strength, such as iron. This concept was also mentioned in Helms et al. (2013a). In a freshwater lake, organically-bound iron was found to be made up of both the large colloidal fraction (from 0.02 µm to 0.45 µm) associated with fulvic acids, as well as the soluble/small colloidal fraction (< 0.02 µm) (Hassler et al. 2009). Shiller (2003) found that almost no DOM was retained on a 0.02 µm filter, and Joung and Shiller (2016) found that most organically-complexed iron is smaller than 0.02 µm. This variability suggests large differences in the processes important in controlling coupled iron and DOM cycling, and requires further investigation in our system.

To address which size fractions of iron and DOM interact, we use sequential filtration to separate DOM and dissolved iron into soluble/small colloidal (<0.02 µm) and large colloidal (0.02 to 0.22 µm) fractions. We then look at the concentrations and proportions of DOC and iron in each size fraction.

(RO 2): Quantify $Fe_{<0.02}$ and DOM concentration controls, seasonality and variability along the aquatic-marine continuum

Riverine DOM dynamics vary widely depending on discharge (Raymond et al. 2016; Wilson et al. 2016; Shultz et al. 2018; Hosen et al. 2019), season (Shultz et al. 2018), land use (Wilson and Xenopoulos 2008), and temperature (Shultz et al. 2018). During high discharge events, more DOM is flushed from the surrounding landscape into rivers and streams, increasing the contribution of allochthonous material (Hood et al. 2006; Fellman et al. 2009; Raymond and Saiers 2010; Yoon and Raymond 2012). Shultz et al. (2018) showed that the concentration of hydrophobic organic acids (HPOA) in the Connecticut River at Middle Haddam increased with increasing discharge, predominantly in the late summer. HPOA has been shown to be composed mainly of lignins bound to carbohydrates (Wershaw et al. 2005), and is an important constituent of allochthonous DOM. Therefore, allochthonous DOM is likely dominant in the late summer and at higher discharge. Given that allochthonous DOM has been suggested to have a higher iron-binding capacity, it's possible that at high discharge (Powell and Wilson-Finelli 2003) and in the late summer, iron concentrations might also be higher compared to other times of the year.

From the perspective of iron export to coastal zones, the transformation of DOM and iron-DOM complexes along a downstream riverine gradient are also of particular importance. In headwaters, DOM tends to have a greater allochthonous contribution, with high contributions of humic acids and a high aromaticity; this is mainly due to a greater connectivity to the terrestrial landscape. Larger rivers are less connected to the terrestrial landscape and have less canopy cover; therefore, contributions of autochthonous DOM may be higher because of greater rates of primary production, particularly in the summer and at low flow, when river residence time increases (Hosen et al. 2019). Furthermore, photochemical and microbial degradation become more important in mainstem sites, which transform and degrade DOM; these processes are also more important during low flow. Therefore, the ability of DOM to complex iron, and subsequently riverine iron concentrations, might also change with changes to DOM composition downstream, though this is largely unexplored. Photoreduction or photooxidation of DOM-bound-iron might also impact its speciation and concentration. Thus variability at the mouth of the Connecticut River is partly driven by variability in upstream processes, which has not been accounted for in past studies.

To address seasonality and variability of $Fe_{<0.02}$ and DOM, we sample 5 sites along a 214 km reach of the Connecticut River mainstem, bi-weekly for 2 years. Three freshwater sites from Northfield, MA to Middle Haddam, CT capture variability in downstream gradients due to DOM photo- and bio-degradation. Middle Haddam is a freshwater tidal site. Two brackish tidal sites at Essex and Old Lyme, CT capture variability in the freshwater-marine continuum. The frequent measurements over a 2-year span and across a range of hydrologic conditions will address the seasonality of iron and DOM concentrations. Capturing the downstream gradient and seasonal variability together will provide a quantitative understanding of the environmental drivers of iron concentration along the aquatic-marine continuum. This is needed for improving estimates of riverine iron fluxes to coastal zones and oceans.

(RO 3): Estimate iron loss at the Connecticut River-Long Island Sound interface due to salinity-induced flocculation

In coastal waters such as estuaries, the loss of dissolved iron and organic matter by flocculation and settling is particularly prominent, due to the changes in salinity and pH from the freshwater riverine environment to the saline marine environment. This causes the flocculation and settling of dissolved and colloidal iron, reducing the riverine export of iron to oceans. However, a small percentage of dissolved and colloidal iron can remain soluble in the estuarine mixing zone due to interactions with DOM, which allows for the export of iron to oceans (Powell and Wilson-Finelli 2003; Krachler et al. 2005). This can occur because iron-DOM complexes are more soluble than inorganic forms of iron, such as iron-hydroxide. Though DOM is also affected by salt-induced flocculation, the amount of DOM lost is less than the amount of inorganic iron (Yang et al. 2017).

Whether iron is able to escape the estuarine mixing zone is dependent on the form of iron involved in the complexation reaction, the type or source of DOM, and the stability of the resulting complex. Krachler, Jirsa, and Ayromlou (2005) found that in a "typical" unpolluted river system draining a predominantly forested area, the percent of the dissolved or colloidal iron that escaped the estuarine mixing zone and was exported to the open ocean was less than 5%. The same study found that a river dominated by DOM inputs from sphagnum peat-bogs exported 20% of its Fe load; this difference was attributed to the difference in DOM source and the resultant variability in quality, which allowed for a greater percentage of iron complexation and stability in the estuarine mixing zone. This is supported by other studies, which have shown the amount of humic or fulvic-like compounds in DOM to be the determining factor in whether DOM is able to escape the estuarine mixing zone (Krachler et al. 2016, 2019).

Because there is both hydrologic and seasonal variability in the source and quality of DOM as well as iron concentrations upstream, we predict the interaction between upstream and in-situ processes acting separately and together on DOM and iron will determine amount of iron escaping the estuarine mixing zone. Some studies have examined the loss of iron in the estuarine mixing zone seasonally and across a variety of hydrologic conditions (Ho et al. 2019), but few have examined the variability of iron and DOM together (Joung and Shiller 2016), and none at high temporal resolutions. To address this, we are sampling the Connecticut River mainstem at Middle Haddam, Essex, and Old Lyme, CT bi-weekly for 2 years. Middle Haddam is a tidal freshwater site that has very little new inputs of DOM from tributaries, Essex is a brackish tidal site, with a relatively low salinity at high tide, compared to Old Lyme, further downstream near the mouth of the Connecticut River, where the salinity is higher at high tide. By comparing iron concentrations at these three stations we can determine the amount of iron lost by salinity-induced flocculation, as well as dilution of high riverine iron concentrations with the low-iron estuarine endmember. This loss is then compared to DOM composition determined using DOM optical parameters, DOC concentrations, and environmental conditions (e.g., discharge, temperature), in order to determine the controls on iron loss and any seasonal or event-based patterns in iron loss.

(RO 4): Provide a conceptual model on the environmental controls on riverine iron export to the Long Island Sound

A conceptual model describing the environmental controls on riverine iron export to the Long Island Sound will be developed using the first three research objectives described above. The model will include differences in behavior of the soluble and colloidal iron fractions (RO #1) in both the watershed, freshwater and brackish riverine sections. This has been addressed elsewhere (Joung and Shiller 2016; Ho et al. 2019), but only for river plumes in estuaries; in freshwater, rarely are the two fractions examined separately, despite evidence that their sources vary (Stolpe et al. 2012). The model will also constrain the controls on freshwater riverine iron concentrations using the variability captured in RO #2; such controls include hydrologic factors (i.e., precipitation and discharge), biogeochemical factors (i.e., DOM source and composition), and biologic factors (i.e., iron uptake). Lastly, the model will evaluate changes to both iron fractions at the freshwater-saltwater interface, and describe the controls on iron loss, addressed in RO #3.

2.3. Methods

2.3.1. Sampling sites

Five sites along a 214 km stretch of the Connecticut River are currently being sampled every other week (Table 2.1; Figure 2.2), starting in July 2018 and continuing until July 2020. At one site, the Connecticut River at Thompsonville, collection began as early as April 2018. As of December 9, 2019, 168 samples in total have been collected. Samples were taken starting at the most upstream site (Northfield), and then the following day the next downstream site (Thompsonville), and so on. The exception was for Old Lyme, which was sampled within 30 minutes of the sampling at Essex. Both Essex and Old Lyme were also sampled within 1 hour of peak high tide. The Connecticut River at Northfield and Thompsonville are freshwater segments. Northfield is predominantly forested with some agriculture, compared to Thompsonville, which has more urban area in its watershed, mainly from Springfield, MA directly upstream. The Connecticut River at Middle Haddam is tidal freshwater; it has little new tributary input compared to Thompsonville, and the residence time from Thompsonville to Middle Haddam is long. The Connecticut River at Essex and Old Lyme are brackish tidal sites, though the salinity at Old Lyme during high tide is higher. The average salinity at Essex is 2.86 PSU (0 to 13 PSU) compared to an average of 15.0 PSU (0 to 28 PSU) at Old Lyme.

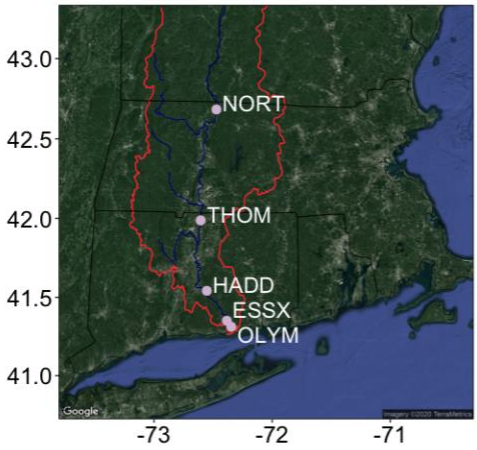

Figure 2.2. Sites along the Connecticut River sampled bi-weekly.

All sites are actively monitored USGS stream gages with stage, temperature, pH, dissolved oxygen, conductivity, turbidity and fluorescent DOM measured every 15 min, and two out of the 5 sites are measured every 15 minutes for discharge (Thompsonville and Middle Haddam). As such, these parameters can be compared to our measured samples at the time of collection. Samples

were collected at all parts of the hydrograph at Thompsonville and Middle Haddam (Figure 2.3), indicating that a wide range of flow conditions are captured in the analysis. Furthermore, as of December 9, 2019, the number of samples taken during each season were 35, 56, 55, and 22, for spring, summer, fall, and winter, respectively.

Table 2.1. Sites along the Connecticut River sampled bi-weekly. Sites are ordered from the most upstream site (Northfield) to the most downstream site (Old Lyme).

Site	Location	USGS ID	Latitude	Longitude	# Samples*
NORT	Northfield, MA	01161280	42.68333	–72.47194	32
THOM	Thompsonville, CT	01184000	41.98722	–72.60583	40
HADD	Middle Haddam, CT	01193050	41.54167	–72.55361	31
ESSX	Essex, CT	01194750	41.35148	–72.38437	30
OLYM	Old Lyme, CT	01194796	41.31250	–72.34639	30

* As of December 9, 2019

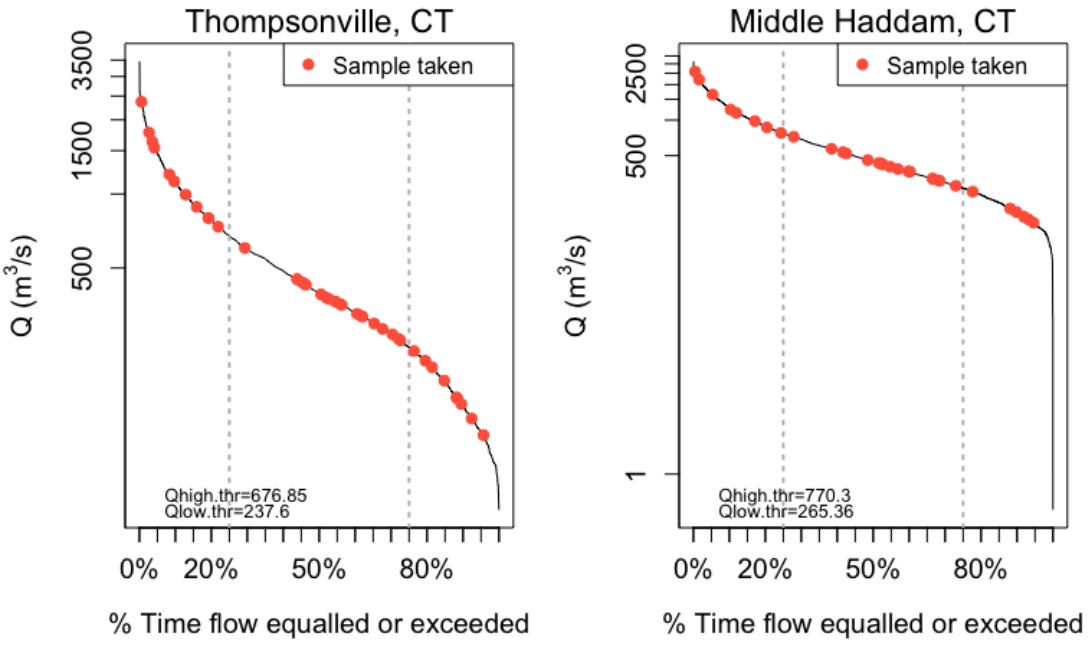

Figure 2.3. Flow exceedance probability for Thompsonville and Middle Haddam. Overlain points denote the discharge at each site when samples were taken. High (25%) and low (75%) thresholds were calculated and plotted for each site, using R v.1.1.463 and the R package HydroTSM.

2.3.2. Sample Collection and Storage

All sample bottles were acid-soaked with 1N HCl for at least 24 hours, and then rinsed 4 times with Milli-Q water. Samples were collected at each site using an acid-rinsed polypropylene bucket or jug, which was rinsed three times with sample water before collection. Samples were filtered on-site through Sterivex 0.22 µm polyethersulfone membrane filters using acid-washed PharMed BPT tubing and a peristaltic pump. Sterivex filters and tubing were purged with at least 250 mL of milli-Q water, and then with at least 50 mL of sample. For Fe(II) collection, an acid-

washed Tygon E-3603 tube was attached to the outlet of 0.22 μm filter, and the tube placed in the bottom of an acid-washed 60 mL amber bottle. The bottle was then over-filled 3 times with the 0.22 μm filtrate, the tube slowly removed, and the bottle capped immediately, ensuring that no air bubbles were trapped inside the sample bottle. This was placed immediately on ice, and then at 4°C in the lab until analysis. For total dissolved/soluble iron and DOM, two 120 mL HDPE bottles were filled with filtrate from the 0.22 μm filter. Both samples were immediately placed on ice in the field and then at 4°C in the lab until subsequent filtration and analysis. Starting in the summer of 2019, unfiltered samples to measure total unfiltered iron were collected at the CT River mainstem sites in 30 mL acid-soaked HDPE bottles, and frozen immediately.

2.3.3. 0.02 μm filtration

Half (~30 mL for ferrous iron and 120 mL for total iron/DOM) of each 0.2 μm sample was sequentially filtered through a Whatman Anopore inorganic membrane (Anodisc) 0.02 μm filter (Whatman # 89203-116). All filtering equipment (e.g., vacuum flask) was acid-soaked in 1 N HCl, rinsed 4 times with milli-Q water, and then baked at 450°C for 5 hours. The sequential filtration of the portion of the 0.2 um filtrate using 0.02 μm filter was conducted on the CT River mainstem samples within 4 days of collection. For each sample, a 0.02 μm filter was placed on the vacuum filtration setup and rinsed with at least 300 mL of milli-Q water, and then with at least 10 mL of sample. Roughly 30 mL of the 0.2 μm Fe(II) filtrate was then 0.02 μm filtered, and Fe(II) was immediately measured on both size fractions (see Section 2.3.4). One of the two HDPE bottles containing 0.2 μm filtrate was then filtered through the 0.02 μm filter on the same vacuum setup, and transferred to a clean 120 mL HDPE bottle. The <0.02 μm fraction is denoted as "small colloidal or soluble," and the 0.02 to 0.22 μm fraction is denoted as "large colloidal," in this study. The 0.02-0.22 μm fraction was calculated by difference (i.e., by subtracting each parameter measured on the 0.02 μm fraction from the 0.22 μm fraction).

2.3.4. Measurements

Fe(II) was measured using the 1,10-phenanthroline method on the Hach DR900 or the Hach FerroVer Pocket Colorimeter II within 4 days of collection and immediately after 0.02 μm filtration. Total iron concentrations were measured using the Hach FerroVer method on the Hach Hach DR900 or the Hach FerroVer Pocket Colorimeter II within 1 month of collection. Standards were prepared before each run according to the Hach FerroVer method sheet (DOC 316.53.01458). Fe(III) concentrations were calculated by subtracting the measured Fe(II) concentrations from the total Fe concentrations.

Dissolved organic carbon (DOC) concentrations were measured the <0.22 and <0.02 μm size fractions as non-purgeable organic carbon (NPOC) on a Shimadzu TOC-V Analyzer within 1 month of collection. Standards and quality checks were measured for each run and were prepared according to Shimadzu protocol.

DOM UV-vis absorption spectra and fluorescence excitation-emission matrices were measured on the <0.22 and <0.02 μm size fractions on a Horiba Aqualog fluorometer.

Chromophoric dissolved organic matter (CDOM), the DOM pool that absorbs light, can be analyzed using absorption parameters, such as the log-transformed absorption slopes from 275 – 295 nm ($S_{275-295}$) and 350 – 400 nm ($S_{350-400}$), and the ratio of the two (slope ratio, S_R). The molecular weight of DOM has been shown to be negatively correlated to S_R (Helms et al. 2008). Hernes (2003) found the absorption coefficient at 350 nm ($a_{CDOM}350$) to be associated with dissolved lignin concentration. The specific UV absorbance at 254 nm ($SUVA_{254}$), which is CDOM absorbance at 254 nm divided by DOC concentration, has been used as a measure of CDOM aromaticity (Weishaar et al. 2003). High molecular weight, high lignin concentration, and aromaticity, are all characteristic of allochthonous DOM. The freshness index (β/α) is the ratio of fluorescence associated with freshly produced DOM vs. that associated with more decomposed DOM, and is indicative of the amount of DOM processing (Parlanti et al. 2000). It was calculated as the ratio of fluorescence emission at 450 and 500 nm, at excitation at 370 nm. The fluorescence index (FI) is a measure of the "source" of the DOM, with a higher fluorescence index indicative of microbial or algal DOM (i.e., autochthonous DOM), and a lower index associated with more terrestrial, plant- or soil-derived DOM (i.e., allochthonous DOM) (Cory and McKnight 2005). It was calculated by dividing the fluorescence emission at 470 nm by 720 nm, at an excitation wavelength of 370 nm.

2.3.5. Ferric iron UV-vis corrections

Fe(III) has been shown to absorb in the UV-vis wavelengths where numerous DOM optical parameters are measured, such as a_{254}, $SUVA_{254}$, and S_R (Weishaar et al. 2003; Poulin et al. 2014). Therefore, Fe(III) corrections on DOM absorption at 254 nm (a_{254}) were performed using Fe(III) concentrations according to Poulin et al. (2014). $SUVA_{254}$ was calculated using the corrected a_{254} values.

2.4. Preliminary Results

2.4.1. Concentration and proportions of DOM and iron in two size classes, using 0.22 and 0.02 μm filters

The average DOC concentration for the 0.22-0.02 and <0.02 μm fractions at all 5 sites was 0.13 and 3.22 mg/L, respectively (Table 2.2). The total Fe concentrations in the 0.22-0.02 and <0.02 μm fractions were 0.070 and 0.017 mg/L, respectively (Table 2.2). Fe(II) in the 0.22-0.02 and <0.02 μm fraction was 0.009 and 0.011, respectively and Fe(III) was 0.061 and 0.011, respectively. DOC in the 0.22-0.02 μm fraction was extremely low (<0.41 mg/L), and very little (4.2%, on average) is removed by 0.02 μm filtration. Conversely, 82.4% of the total Fe is removed by filtration through 0.02 μm, and only 17.62% of total Fe passes through the small fraction. Because of the extremely small difference between DOC in the 0.02 and 0.22 μm fractions, the difference in optical measurements were also extremely low, and in the noise range (i.e., sometimes negative). As such, these values were not averaged or included in Table 2.2.

Table 2.2. Results of various parameters, measured or calculated by difference (0.22-0.02) for each size fraction.

	< 0.22	0.22 – 0.02	< 0.02
DOC (mg/L)	3.31 (2.05 to 6.48)	0.13 (0.004 to 0.41)	3.22 (2.08 to 6.74)
Total Fe (mg/L)	0.087 (0.002 to 0.255)	0.070 (0 to 0.193)	0.017 (0 to 0.110)
Fe(II) (mg/L)	0.020 (0 to 0.067)	0.009 (0 to 0.028)	0.011 (0 to 0.044)
Fe(III) (mg/L)	0.068 (0 to 0.212)	0.061 (0 to 0.183)	0.011 (0 to 0.067)
a_{254} (m^{-1})	11.00 (6.10 to 26.88)		10.14 (5.67 to 24.76)
$SUVA_{254}$ (L $mg^{-1}m^{-1}$)	3.36 (2.29 to 4.29)		3.16 (2.13 to 4.04)
FI	1.52 (1.46 to 1.63)		1.53 (1.45 to 1.62)
β/α	0.59 (0.43 to 0.77)		0.60 (0.43 to 0.93)
S_R	0.80 (0.66 to 1.19)		0.82 (0.64 to 1.09)

2.4.2. Quantify $Fe_{<0.02}$ and DOM concentration controls, seasonality and variability along the aquatic-marine continuum

For the three upstream sites, Northfield, Middle Haddam, and Thompsonville, seasonally, summer and fall had significantly higher $DOC_{<0.02}$ concentrations than the winter and spring ($P < 0.01$) with an average of 3.50 and 3.85 mg/L in the summer and fall, respectively, and 2.43 and 3.06 in the winter and spring, respectively. The type of DOM also varied seasonally; β/α was greater in the summer than any other season ($P < 0.01$), with an average of 0.63 (s.d. = 0.049) in the summer and 0.577 (s.d. = 0.050) for all other seasons. There were no significant trends in $SUVA_{254}$ seasonally, except for marginally significant greater $SUVA_{254}$ in the fall compared to the winter ($P = 0.067$); $SUVA_{254}$ was, on average, 3.44 L mgC^{-1} m^{-1} in the fall compared to 3.17 L mgC^{-1} m^{-1} in the summer. Overall, the fall had a significantly greater contribution of $Fe_{<0.02}$ than both spring and summer ($P < 0.01$), with an average concentration of 0.031 mg/L (s.d. = 0.021) in the fall compared to 0.014 mg/L in both the spring (s.d. = 0.006) and summer (s.d. = 0.022).

For the three upstream sites, Northfield, Middle Haddam, and Thompsonville, there was no relationship between total Fe, Fe(II), or Fe(III) and DOC in the 0.22-0.02 fraction ($R^2 < 0.02$, $P > 0.1$, data not shown). However, we observed relationships between $Fe_{<0.02}$ and $DOC_{<0.02}$, $SUVA_{254\,<0.22}$, $S_{R\,<0.02}$, and $\beta/\alpha_{<0.02}$ (Figure 2.4). These relationships were stronger for each season individually. For example, for $Fe_{<0.02}$ and $DOC_{<0.02}$ (Figure 2.4a), there were strong positive correlations in the summer, fall, and winter ($R^2 = 0.75$, 0.47, and 0.58, respectively), and a negative correlation in the spring ($R^2 = 0.39$). For $Fe_{<0.02}$ and $SUVA_{254\,<0.22}$ (Figure 2.4b), there was a negative correlation in the spring ($R^2 = 0.4$, $P = 0.022$), strong positive relationships in the summer and fall ($R^2 = 0.73$ and 0.62, respectively, $P < 0.01$), and a weak positive relationship in the winter ($R^2 = 0.24$, $P = 0.042$). For $Fe_{<0.02}$ and $S_{r\,<0.02}$ (Figure 2.4c), there was no relationship in the spring and winter, but negative correlations in the summer and fall ($R^2 = 0.63$ and 0.36, respectively, $P < 0.01$). For $Fe_{<0.02}$ and $\beta/\alpha_{<0.02}$ (Figure 2.4d), there was a weak positive correlation in the spring ($R^2 = 0.011$, $P = 0.081$), negative correlation in the summer and fall ($R^2 = 0.48$ and 0.49, respectively, $P < 0.01$), and no relationship in the winter. Furthermore, when $\beta/\alpha_{<0.02}$ was greater than ~0.63,

$Fe_{<0.02}$ was consistently close to 0 (0.00096 mg/L, on average, ranging from 0 to 0.01 mg/L); the freshness index was only greater than 0.63 in the summer and fall.

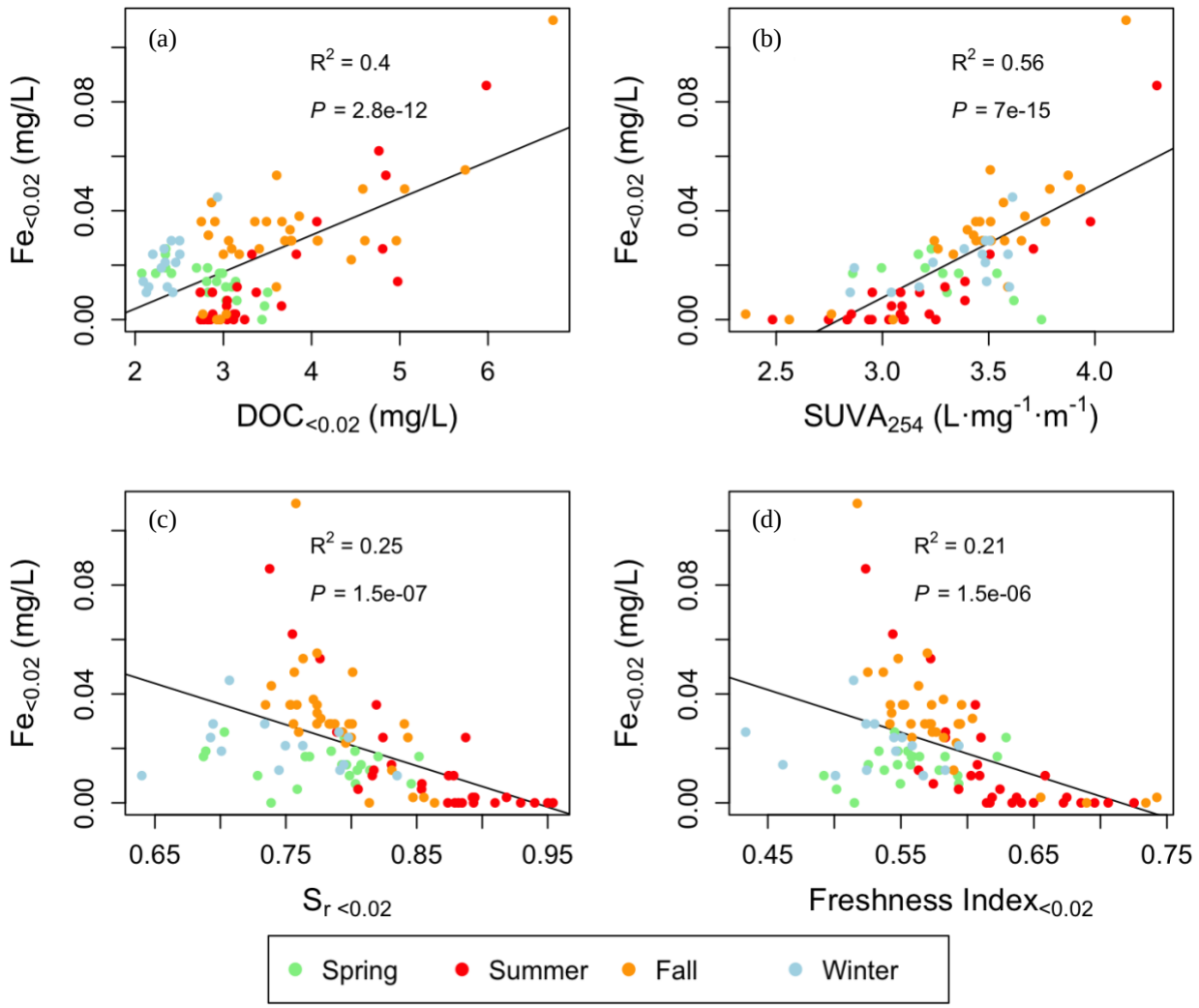

Figure 2.4. $Fe_{<0.02}$ in the freshwater sites Northfield, Thompsonville, and Middle Haddam vs. (a) $DOC_{<0.02}$, (b) $SUVA_{254\ <0.22}$, (c) S_R, and (d) the freshness $index_{<0.02}$. Seasons are denoted by color. R^2 and P values are for all seasons combined.

The freshness index and S_R were both negatively correlated to the natural log of the discharge at Thompsonville (R^2 = 0.51 and R^2 = 0.45, respectively, $P < 0.01$) and Middle Haddam (R^2 = 0.53 and R^2 = 0.42, respectively, $P < 0.01$). $SUVA_{254}$ showed only a weak positive correlation with discharge at Thompsonville and Middle Haddam (R^2 = 0.11 and R^2 = 0.25, respectively, $P < 0.01$). At low discharge (< 237.6 m^3/s at Thompsonville and < 265.4 m^3/s at Middle Haddam), the average $Fe_{<0.02}$ was 0.0009 mg/L, with a max concentration of 0.005 mg/L (n = 15). The average $Fe_{<0.02}$ for discharge 25-75% was 0.026 mg/L with a max of 0.11 mg/L (n = 37), and for high discharge, the average was 0.025 mg/L, with a max of 0.086 mg/L (n = 19). The $Fe_{<0.02}$ concentration at low discharge was significantly lower than the other two discharge regimes ($P < 0.01$), while there was no significant difference between the 25-75% regime and the high discharge regime (Figure 2.5a). There was no significant difference in $Fe_{0.22\text{-}0.02}$ concentration

between high and low discharge, though $Fe_{0.22\text{-}0.02}$ in the 25-75% discharge regime was significantly higher than both high and low discharge (data not shown, $P < 0.01$). On average, $SUVA_{254}$ was 2.86 L mgC^{-1} m^{-1} at low discharge, compared to 3.44 L mgC^{-1} m^{-1} at 25-75% and high discharge together. The difference between low discharge and the other two regimes was significant ($P < 0.01$), while there was no significant difference between 25-75% and high discharge (Figure 2.5b). The freshness index also showed significant differences between flow patterns, with a significantly lower freshness index with each increasing flow regime (Figure 2.5c, $P < 0.01$).

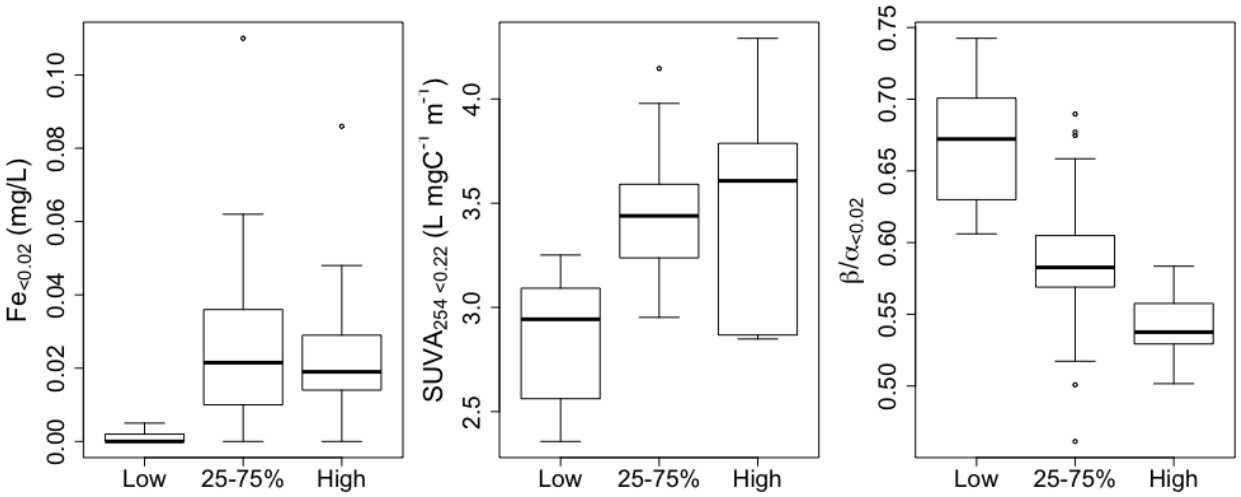

Figure 2.5. (a) $Fe_{<0.02}$, (b) $SUVA_{254\ <0.22}$, and (c) the freshness index$_{<0.02}$ for three different discharge regimes at Thompsonville and Middle Haddam, combined.

2.5. Preliminary Discussion

Since most (> 95%, on average) of the DOC in the <0.22 μm fraction is also present in the <0.02 μm fraction, any iron bound to DOC would also need to be present in the <0.02 μm fraction. This is supported by past studies, which have found that very little DOM is retained by a 0.02 μm filter (Shiller 2003), and that iron-DOM complexes were mostly present in the <0.02 μm fraction (Joung and Shiller 2016). Since roughly 82.4% of total iron is removed by 0.02 μm filtration, this also suggests that the majority of the iron in Connecticut River is not organically-complexed; however, from the perspective of iron export, it is the organically-complexed iron fraction, however small, that is most important. Therefore, to evaluate the cycling of organically-complexed iron in tandem with DOC, we focused on the <0.02 μm size fraction.

$Fe_{<0.02}$ concentrations are to some extent driven by DOM quality and quantity. The strong relationship between $SUVA_{254}$ and $Fe_{<0.02}$ (Figure 2.4b) suggests that the aromaticity of DOM may be an important factor in controlling $Fe_{<0.02}$ concentrations, and that aromaticity might be an indicator of DOM iron-binding capacity, as has been shown in past studies for iron and other metals (Baken et al. 2011; Kikuchi et al. 2017; Xu et al. 2018). Stolpe et al. (2012) also found that when allochthonous aromatic DOM loads were high, small fulvic-rich iron colloids were present

at higher concentrations. In the fall and late summer in particular, the relationship between $Fe_{<0.02}$ and DOC concentrations and $Fe_{<0.02}$ and $SUVA_{254}$ is particularly strong. This is likely because both the source of aromatic DOM is the same as the source of $Fe_{<0.02}$ (e.g., soil) (Norrström 1995; Stolpe et al. 2012), and that an increase in the amount of aromatic DOM results in an overall higher iron-binding capacity which supports higher riverine $Fe_{<0.02}$ concentrations (Baken et al. 2011; Fujii et al. 2014). Our observed increase in allochthonous DOM in the late summer and fall is supported by Shultz et al. (2018), and the subsequent increase in $Fe_{<0.02}$ is in line with our hypothesis that $Fe_{<0.02}$ will be driven by allochthonous DOM. Greater dissolved iron concentrations in the fall are also supported by past studies, such as in Shiller (1997), though Shiller (1997) suggested that changes in redox conditions was the cause of the observed seasonal variability in $Fe_{<0.02}$.

S_R and the freshness index, which are proxies for DOM molecular weight and the proportion of recently-produced DOM to degraded DOM respectively, both had thresholds above which $Fe_{<0.02}$ concentrations were close to 0. These thresholds were mostly exceeded in the summer and occasionally the fall and when discharge was low (i.e., close to or below 237.6 m^3/s and 265.4 m^3/s for Thompsonville and Middle Haddam, respectively). In these instances, $Fe_{<0.02}$ was consistently close to 0 (Figure 2.4c-d and Figure 2.5a and c). There are a couple of potential explanations for this. Firstly, at low discharge there is a greater contribution of groundwater and less interaction with the terrestrial landscape. This results in a lower contribution of allochthonous DOM, and therefore, less $Fe_{<0.02}$ (regardless of its source) can be bound to DOM and remain in solution. Given that $SUVA_{254}$ was significantly lower at low discharge and that DOM aromaticity is a driving factor of iron-binding capacity (Baken et al. 2011; Fujii et al. 2014), lower inputs of allochthonous aromatic DOM at low flow is likely a contributing factor to low $Fe_{<0.02}$ in the summer. Furthermore, given that $Fe_{<0.02}$ also likely has the same source as allochthonous DOM (e.g., soil) (Norrström 1995; Stolpe et al. 2012), it would also mean less $Fe_{<0.02}$ entering directly. Secondly, at low discharge, primary production has been shown to increase, and primary production has also been shown to be positively correlated to both S_R and β/α (Hosen et al. 2019); with greater primary production, there is a greater potential for iron uptake, which could reduce $Fe_{<0.02}$ concentrations. The lack of relationship between $Fe_{<0.02}$ and either S_R and β/α in the winter and spring, when primary production is a less important process, indicate that it's likely that uptake by primary producers also plays a role in low iron concentrations in the summer.

2.6. Next Steps

Sampling will continue bi-weekly at all 5 sites until July 2020, completing the two year dataset. Supplies are funded through a Yale Institute for Biospheric Studies grant. For each sample and size fraction, about 60 mL of filtrate is archived and stored frozen, in case additional measurements should be made. Preliminary results and analysis showed the coupling of $Fe_{<0.02}$ and $DOC_{<0.02}$, with an important seasonal component. How this will impact iron export to the Long Island Sound needs to be evaluated further. As such, additional focus will be placed on addressing RO #3 and RO #4, as described in Section 2.2Research Objectives. In the summer 2020, mixing

experiments with different riverine endmembers (i.e., Connecticut River mainstem, smaller tributaries) and the estuarine endmember (Old Lyme at high tide) will also be conducted in order to determine whether the loss of $Fe_{<0.02}$ from the freshwater to estuarine endmember is conservative or non-conservative, and whether the loss can be directly related to differences in DOM quality or quantity, such as the fluorescence index.

3. Illuminating riverine DOC dynamics using carbon age

3.1. Introduction and Significance

Understanding the global carbon cycle is essential to predicting future climate change. Dissolved organic carbon (DOC) is one of the largest carbon reservoirs globally; the amount of carbon stored in oceans alone as DOC exceeds the amount of CO_2 in the atmosphere (Cubasch et al. 2013), and the amount of organic carbon stored in soils is also greater than the atmospheric carbon pool (Schlesinger and Bernhardt 2013). Despite its known importance in the global carbon cycle, DOC is also a significant source of uncertainty. DOC leaches from organic matter stored in plants, plant litter, and soils. It can then be exported into rivers from the surrounding landscape, where it can be transported to oceans (Raymond et al. 2016), transformed, respired and evaded (Battin et al. 2008, 2009). While the flux of DOC from rivers to oceans is fairly well-constrained at about 0.4 x 10^{15} g of organic carbon (both particulate and dissolved) annually (Meybeck 1982; Raymond and Spencer 2015), the ultimate source and lateral transport of DOC from the terrestrial landscape to rivers is uncertain. This is because DOC is difficult to measure directly, and its sources vary on timescales ranging from hours to years, due to hydrologic and biologic factors, landscape properties, and climate. Sampling infrequently or only during certain seasons creates a bias in our understanding of DOC lateral transport, and can make predicting changes to the global carbon cycle challenging.

One indicator of DOC source is its age, which can be measured using the isotopic signature of ^{14}C. Atomic bomb-testing in the 1950s and 1960s led to the enrichment of ^{14}C in the atmosphere. This ^{14}C is then incorporated into plant biomass and eventually soils (O'Brien 1986). Younger organic matter (i.e., post bomb-testing) is then enriched in ^{14}C compared to aged organic matter, which is more depleted in ^{14}C. In general, rivers have been shown to export modern carbon (> 1950) from recently dead plant organic matter and surface soils (Hedges et al. 1986). However, DOC in rivers can be older if it originates from deeper soils, groundwater, or peatlands, for example. In fact, the range of organic matter age in the top meter of soil is from modern to more than 5000 years old (Raymond and Bauer 2001a), which suggests the potential for a large amount of variability in DOC age in rivers with small changes to hydrology. It also indicates the potential mobilization of sequestered carbon stocks in rivers; DOC that was once "removed" from the global carbon cycle (i.e., stored in carbon sinks) that could be laterally exported to rivers could potentially be respired or photochemically oxidized and evaded to the atmosphere, thus contributing to global carbon dioxide emissions. This has serious implications, since according to the IPCC (2013), 1500-2000 PgC is stored in soils and 1.7 PgC/yr is exported from soils to rivers globally (as both organic and inorganic carbon). Even if the lateral flux of DOC from terrestrial landscapes to rivers does not change, a change in the source from young, freshly-produced DOC to older, sequestered DOC may mean a decrease in the organic carbon soil sink.

3.2. Research Objectives and Hypotheses

3.2.1. Research objectives

DOC source, and therefore age, is driven by a variety of complex factors including land use, lithology, hydrology, biology, temperature and climate. The interaction of these factors results in a large amount of within and across system variability that creates uncertainty in predictions of DOC lateral export from terrestrial landscapes to rivers. To predict whether there are long-term changes in DOC age due to factors such as climate change or land use change, long-term measurements of DOC age are necessary; however, high temporal resolution is also essential to capture seasonal and event-based variability in DOC source and age. Here, I propose the continued measurement of ^{14}C-DOC in the Connecticut River, for which we already have data from 2009 and 2015-2018; under the proposed project I will sample at a higher temporal resolution (bi-weekly) over 2 years to account for seasonal and event-based variation in DOC age. The project has 3 main research objectives (ROs), described below.

(RO 1): Derive an age and flux of DOC exported by the Connecticut River

Aged DOC has already been observed in river systems; however, there is a large amount of variability in DOC age within and across river systems, as DOC source and age is dependent on a variety of factors. Raymond and Bauer (2001) found that DOC in the Hudson River was more than 1000 years old. The Susquehanna and Rappahannock Rivers also had older carbon, but DOC in the Amazon, York, Potomac and James Rivers were more modern (Raymond and Bauer 2001b). This difference was attributed to differences in landscape properties, with the Hudson River having a large percentage of agricultural land in its watershed; in agriculture, deeper soils are tilled and brought to the surface, which could mobilize aged DOC. This idea was supported by Butman et al. (2015), which showed that DOC in temperate rivers was older in watersheds that had more human disturbance (i.e., greater percentage of urban or cultivated land) and a higher population. While inputs of fossil fuel based organic carbon (i.e., wastewater, synthetic fertilizers, or direct inputs) likely contribute to the increase in DOC age observed with increasing urbanization and cultivation to some extent (Griffith and Raymond 2011), Butman et al. (2015) suggests that the predominant driver of increasing riverine DOC age is the mobilization of older soil organic carbon stocks. Watershed lithology also plays an important role in the age of DOC in rivers; Raymond et al. (2004) found that aged DOC was only found in temperate river systems underlain by organic matter rich sedimentary rocks, such as black shale. This suggests at least some contributions of aged sedimentary carbon to the aged riverine DOC pool.

The age of riverine DOC has also been shown to vary with climate and season. Qu et al. (2017) found aged DOC in rivers in the Tibetan Plateau were likely to be sourced from permafrost soils, and that the mobilization of this older soil carbon was likely due to warming temperatures and permafrost thaw. Aiken et al. (2014), however, found that DOC age was negatively correlated to permafrost area, and that peat was a source of younger DOC compared to other sources such as groundwater. This was also supported by Striegl et al. (2007), which found aged DOC at all river

sites except the one with a wetland-dominated watershed. In arctic rivers, riverine DOC was older in the summer and fall compared to the spring (Striegl et al. 2007; Aiken et al. 2014). This was attributed to greater contributions of DOC from groundwater and melting glaciers, thus suggesting that hydrology plays an important role in DOC age. Some studies have shown greater contributions of aged riverine DOC at higher discharge (Butman et al. 2012; Qu et al. 2017) and others at lower discharge (Raymond et al. 2007; Butman et al. 2012, 2015). This variability is due to the unique hydrologic and biological drivers in different climates and river systems, and stresses the importance of addressing this question in the Connecticut River.

Once in rivers, DOC composition and age can change due to in-stream DOC transformation reactions or the addition of DOC through primary production. In situ production of DOC has been shown to contribute to some of the observed variability in DOC age (Raymond and Bauer 2001a), resulting in an overall more modern signature. On the other hand, simultaneous in-stream DOC bio-degradation results in an overall older DOC signature, due to the preferential removal of younger DOC (Raymond and Bauer 2001b). Therefore, the age of carbon being exported to oceans by rivers is determined both by the age of the DOC source material and the simultaneous downstream production and degradation of DOC. This means that the age of DOC being exported to oceans is likely different from the age of its terrestrial source (Raymond and Bauer 2001b).

From the perspective of the global carbon cycle, both the flux and age of DOC are important, as the flux will provide information on the quantity of DOC in rivers and the age will provide information on the source. Furthermore, both the lateral terrestrial flux and the riverine flux to estuaries and oceans are important. To determine the average flux and age of DOC in the Connecticut River, we will sample the Connecticut River at Thompsonville, CT, bi-weekly for 2 years, to account for seasonal and event based variability. An annual flux and average age will be estimated. The average DOC age and lateral export from the terrestrial environment to the river will be estimated using the model developed by Hosen et al. (*in review*), which separates the terrestrially-sourced and in-situ DOC pools based on river discharge. All these values can inform modeling efforts, since what can be learned about the Connecticut River can be applied to other temperate river systems.

(RO 2): Determine whether there is a long-term trend towards older DOC in the Connecticut River

Some studies have shown changes to DOC age that are driven by long-term factors such as climate change (Qu et al. 2017) or land use (Butman et al. 2015). Furthermore, long-term ^{14}C-DOC measurements in a particular system can be used to determine whether carbon cycling in that system is in a steady-state (i.e., in equilibrium with the atmosphere); a system in a steady state would indicate that the riverine DOC pool originated recently, and thus that there is a balance between CO_2 fixation by primary producers (e.g., plants or algae) and the transport of that fixed carbon in rivers.

In the 1950s and 1960s, nuclear testing led to a huge spike of ^{14}C, known "bomb-^{14}C", into the atmosphere; ^{14}C in the atmosphere has been decreasing at a steady state ever since. A river

system that is in equilibrium with the atmosphere would show a similar slope of decrease in $\Delta^{14}C$, due to the incorporation of the present atmospheric $\Delta^{14}C$ level into new plant biomass, and ultimately that organic matter containing the same $\Delta^{14}C$ signature into rivers. A deviation from this slope indicates non-steady-state behavior, and the mobilization of older, sequestered carbon stocks (Figure 3.1). Therefore, to determine whether there is truly a *shift* to older DOC sources in a particular system, long-term measurements are essential.

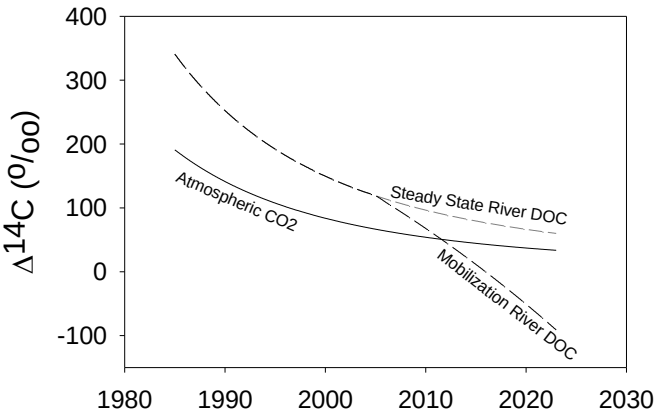

Figure 3.1. Model showing steady state river DOC compared to mobilization river DOC. From Raymond (2019).

No studies have reported performing this analysis for ^{14}C-DOC. However, Mayorga et al. (2005) performed this analysis for $\Delta^{14}C$-CO_2 outgassed from the Amazonian river system. They found that the change in $\Delta^{14}C$-CO_2 over a 7 year period was about the same as the change in $\Delta^{14}C$-CO_2 in the atmosphere during that same time period (Figure 3.2), which suggested the respiration of freshly produced organic carbon (i.e., recently photosynthetically sequestered) as opposed to the respiration of aged, sequestered organic carbon. The same approach can be applied to DOC in our river system. Whether aged DOC is being mobilized on the Connecticut River will be addressed by comparing ^{14}C-DOC measurements from 2018 to 2020 to past measurements made in 2009 and 2015-2018 at the same site. This change over time will be compared to the change of atmospheric $\Delta^{14}C$-CO_2, as demonstrated in Figure 3.1 and Figure 3.2.

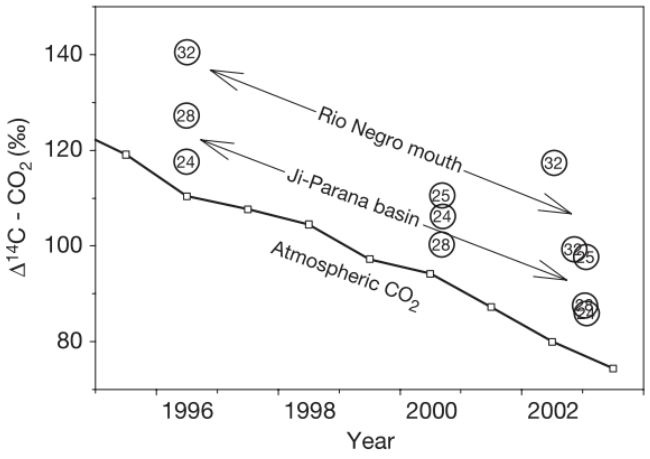

Figure 3.2. $\Delta^{14}C$-CO_2 outgassed over a 7 year period from two rivers in the Amazonian River system. This is compared to the $\Delta^{14}C$-CO_2 of the atmosphere to determine whether CO_2 outgassing is in equilibrium with the atmosphere, or whether there is a mobilization of aged carbon stocks being respired as CO_2. From Mayorga et al. (2005).

3.2.2. Hypotheses

Based off of these research objectives, I hypothesize that:

(1) DOC will be, on average, ^{14}C-DOC enriched (i.e., modern) in the Connecticut River, but that this will vary seasonally, with more depleted ^{14}C-DOC in the summer compared to the spring.

(2) The overall DOC flux will be greatest in the spring, when discharge is high, but the flux of *aged* DOC will be greatest in the summer, when the contribution of aged DOC is higher.

(3) There will be a long-term trend towards more depleted ^{14}C-DOC in the Connecticut River, which will be driven by an increase in extreme discharge events (droughts and storms) and a trend towards increasing watershed urbanization and cultivation.

3.3. Methods

3.3.1. Sampling Sites

We have been sampling the Connecticut River at Thompsonville, CT (Figure 3.3) bi-weekly beginning in July 2018. Sample collection will end in July 2020. The Connecticut River at Thompsonville has a drainage area of 25019 km^2, and is predominantly forested (88.7%), with a significant urban contribution (6.2%). Agriculture and wetlands make up < 2% of the total watershed area (Butman et al. 2012). The average precipitation is roughly 1141 mm/yr (Butman et al. 2012).

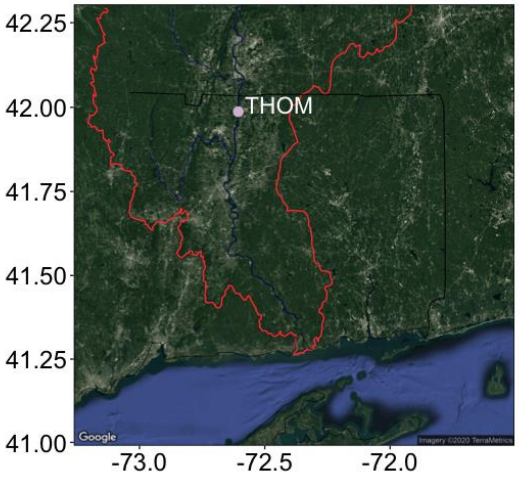

Figure 3.3. Two sites being sampled bi-weekly along the Connecticut River mainstem at Thompsonville, CT (THOM) and Essex, CT (ESSX).

Measurements at this site will be used to determine the average age of DOC in the Connecticut River (RO 1), the lateral flux from the terrestrial landscape to the Connecticut River (RO 1), long-term trends in DOC age (RO 2), and environmental controls on DOC age (e.g., hydrology). The Connecticut River at Thompsonville is a USGS stream gage location (USGS ID 01184000), so gage height, discharge, pH, temperature, dissolved oxygen, conductivity and turbidity are measured every 15 min, and these values can be compared to our grab samples.

The Raymond lab already has 4 years of ^{14}C-DOC measurements at the Connecticut River at Thompsonville that the proposed measurements will be compared to in order to determine long-term trends (n = 27). Samples collected at this site and run for ^{14}C-DOC from 2015 to 2018 are described in Table 3.1. During this time frame, only 2016 had at least one measurement for all 4 seasons. In 2015, samples were only collected and measured for ^{14}C-DOC in the summer and fall, and in 2017, measurements were made for ^{14}C-DOC in the winter, spring, and summer, but not the fall. In 2018, only late summer and fall ^{14}C-DOC measurements were made. Samples run for ^{14}C-DOC from 2015 to 2018 already covered a wide range of discharge conditions, but including the samples that have already been collected starting in July 2018 allow for an even more thorough range (Figure 3.4). Furthermore, five samples from the Connecticut River at Thompsonville were measured for ^{14}C-DOC in 2009 in winter, summer and fall, and are described in Butman et al. (2012).

Table 3.1. Samples collected and run for ^{14}C-DOC at Thompsonville, CT from 2015 to 2018, by season. In total, 27 samples were collected over the time period.

Season	Number of samples (*n*)
Spring	5
Summer	8
Fall	8
Winter	6

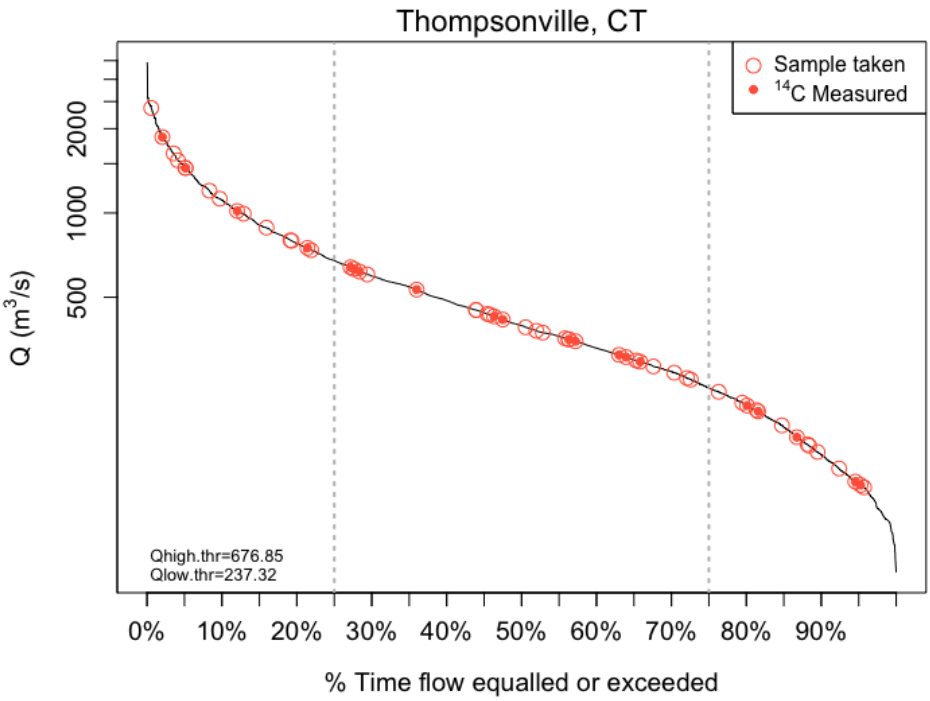

Figure 3.4. Flow exceedance probability for the Connecticut River at Thompsonville, CT. Overlain empty points denote the discharge at each site when samples were taken. Filled points within the empty points indicate samples from 2015 to 2018 in which ^{14}C-DOC has already been measured on the samples. High (25%) and low (75%) thresholds were calculated and plotted for each site, using R v.1.1.463 and the R package HydroTSM.

3.3.2. Sample collection and storage

Samples are collected at each site using an acid-rinsed polypropylene bucket or jug, which is rinsed three times with sample water before collection. Samples are filtered on-site through Sterivex 0.22 μm filters using acid-washed PharMed BPT tubing and a peristaltic pump. Sterivex filters and tubing are purged with at least 250 mL of milli-Q water, and then with at least 50 mL of sample. Samples are then filtered into 120 mL HDPE sample bottles, which were acid-soaked with 1N HCl for at least 24 hours, and then rinsed 4 times with Milli-Q water. Filtrates are frozen within one month of collection and stored at 4°C until then. Frozen samples will be thawed at 4°C at a later date for conversion to CO_2 for ^{14}C analysis, described in Section 3.3.3.

3.3.3. Conversion of DOC to CO_2 for ^{14}C analysis

Either chemical or UV-oxidation is used to convert DOC to CO_2 for ^{14}C analysis, both of which I have experience with. The Raymond Lab has a UV-oxidation chamber connected to a

vacuum line to trap DOC as CO_2. The methods have been previously reported (Butman et al. 2012). Briefly, the sample is placed in a large quartz reactor, acidified to remove dissolved inorganic carbon, and sparged using helium. The sample is then UV irradiated for 6 hours in a UV oxidation chamber, which converts the DOC to CO_2. The CO_2 from the sample is then transferred to the vacuum line using helium. Other gases and any moisture is removed from the vacuum line with a dry ice and propanol "slush," so the CO_2 is cryogenically purified. A liquid nitrogen trap on a tip-off (a hollow Pyrex tube) freezes and traps the CO_2. The tip-off is then flame sealed. These tip-offs will be shipped for accelerator mass spectrometry (AMS) analysis at the Woods Hole Oceanographic Institution (WHOI) National Ocean Sciences Accelerator Mass Spectrometry (NOSAMS) facility.

3.3.4. Carbon age calculations from ^{14}C values

AMS outputs ^{14}C, ^{13}C, and ^{12}C values for each sample. These will be used to calculate carbon age and $\Delta^{14}C$, described below. First, the fraction modern (Fm) is calculated. Fm is defined as a measurement of the deviation of $^{14}C/^{12}C$ from "modern," where modern is defined as 95% of the radiocarbon concentration in 1950 of NBS oxalic acid, normalized to $\delta^{13}C = -19$ ‰ (OLSSON 1970). The Fm is also corrected for natural isotope fractionation by normalizing Fm to –25‰ using $\delta^{13}C$. Radiocarbon age is then calculated using the $\delta^{13}C$-corrected Fm, and the following equation, where –8033 is the mean lifetime of ^{14}C:

$$Age = -8033 \ln(Fm)$$

The $\Delta^{14}C$ value is defined as the relative difference between the absolute international standard in the year 1950 and sample activity corrected for age and $\delta^{13}C$. It is corrected for the time between sample collection and sample measurement, to account for ^{14}C decay during that time period. As such, $\Delta^{14}C$ values made on the same sample during different years will have the same value. Positive values of $\Delta^{14}C$ indicate modern samples, and negative values indicate ages before 1950. It is calculated using the following equation (Woods Hold Oceanographic Institute 2018), where λ is 1/(mean life of ^{14}C) = 1/8267 yrs and y_c is the year of collection:

$$\Delta^{14}C = \left(Fm * e^{\lambda(1950-y_c)} - 1\right) * 1000$$

3.3.5. DOC concentration and UV-vis absorption and fluorescence measurements

To determine the flux of DOC being exported by the Connecticut River, DOC concentrations will be measured as non-purgeable organic carbon (NPOC) on a Shimadzu TOC-V Analyzer within 1 month of collection. Standards and quality checks are measured for each run and are prepared according to Shimadzu protocol.

DOC optics will also be measured to compare other carbon quality indices to the carbon age measurement. This will also help in the determination of terrestrially-sourced DOC vs. in situ DOC. Samples for DOC optics and concentrations will be stored in acid-soaked and Milli-Q rinsed HDPE bottles at 4°C until analysis, for no more than 2 weeks. DOM UV-vis absorption spectra and fluorescence excitation-emission matrices are measured on a Horiba Aqualog fluorometer. Chromophoric dissolved organic matter (CDOM), the DOM pool that absorbs light, can be

analyzed using absorption parameters, such as the log-transformed absorption slopes from 275 – 295 nm ($S_{275-295}$) and 350 – 400 nm ($S_{350-400}$), and the ratio of the two (slope ratio, S_R). The molecular weight of DOM has been shown to be negatively correlated to S_R (Helms et al. 2008). Hernes (2003) found the absorption coefficient at 350 nm ($a_{CDOM}350$) to be associated with dissolved lignin concentration. The specific UV absorbance at 254 nm ($SUVA_{254}$), which is CDOM absorbance at 254 nm divided by DOC concentration, has been used as a measure of CDOM aromaticity (Weishaar et al. 2003). High molecular weight, high lignin concentration, and aromaticity, are all characteristic of allochthonous DOM. The freshness index (β/α) is the ratio of fluorescence associated with freshly produced DOM vs. that associated with more decomposed DOM, and is indicative of the amount of DOM processing (Parlanti et al. 2000). It was calculated as the ratio of fluorescence emission at 450 and 500 nm, at excitation at 370 nm. The fluorescence index (FI) is a measure of the "source" of the DOM, with a higher fluorescence index indicative of microbial or algal DOM (i.e., autochthonous DOM), and a lower index associated with more terrestrial, plant- or soil-derived DOM (i.e., allochthonous DOM) (Cory and McKnight 2005). It is calculated by dividing the fluorescence emission at 470 nm by 720 nm, at an excitation wavelength of 370 nm.

3.4. Timeline and Funding

Sample collection will end in July 2020. During the summer 2020, DOC samples will be converted to CO_2 using the vacuum line method described in 3.3.3. and will be shipped for analysis at WHOI NOSAMS by November 2020. The project is funded by the NASA CT Space Grant ($8000), awarded in October 2019, the bulk of which will be used for WHOI's sample fee. The cost breakdown is described in Table 3.2.

Table 3.2. Budget breakdown for ^{14}C-DOC sample collection and analysis at WHOI NOSAMS.

Budget Category	Item	Per Unit	# Units	Amount
Supplies	0.22 μm filters (50/pk)	$235	1	$235
Travel	Zipcar rental	$88	13	$1,144
Other expenses	NOSAMS	$165	40	$6,600
			Total	$7,979

4. References

Abadie C, Lacan F, Radic A, et al (2017) Iron isotopes reveal distinct dissolved iron sources and pathways in the intermediate versus deep Southern Ocean. Proc Natl Acad Sci 114:858–863 . doi: 10.1073/pnas.1603107114

Aiken GR, Spencer RGM, Striegl RG, et al (2014) Influences of glacier melt and permafrost thaw on the age of dissolved organic carbon in the Yukon River basin. Global Biogeochem Cycles 525–537 . doi: 10.1002/2013GB004764.Received

Baalousha M, Kammer FVD, Motelica-Heino M, et al (2006) Size-based speciation of natural colloidal particles by flow field flow fractionation, inductively coupled plasma-mass spectroscopy, and transmission electron microscopy/X-ray energy dispersive spectroscopy: Colloids-trace element interaction. Environ Sci Technol 40:2156–2162 . doi: 10.1021/es051498d

Baalousha M, Maniculea A, Cumberland S, et al (2008) Aggregation and surface properties of iron oxide nanoparticles: influence of pH and natural organic matter. Environ Toxicol Chem 27:1875–1882

Baken S, Degryse F, Verheyen L, et al (2011) Metal complexation properties of freshwater dissolved organic matter are explained by its aromaticity and by anthropogenic ligands. Environ Sci Technol 45:2584–2590 . doi: 10.1021/es103532a

Battin TJ, Kaplan LA, Findlay SEG, et al (2008) Biophysical controls on organic carbon fluxes in fluvial networks. Nat Geosci 1:95–101 . doi: 10.3354/meps08336

Battin TJ, Luyssaert S, Kaplan LA, et al (2009) The boundless carbon cycle. Nat Geosci 2:598–600 . doi: 10.1038/ngeo618

Benedetti MF, Milne CJ, Kinniburgh DG, et al (1995) Metal Ion Binding to Humic Substances: Application of the Non-Ideal Competitive Adsorption Model. Environ Sci Technol 29:446–457 . doi: 10.1021/es00002a022

Boyle EA, Edmond JM, Sholkovitz ER (1977) The mechanism of iron removal in estuaries. Geochim Cosmochim Acta 41:1313–1324 . doi: 10.1016/0016-7037(77)90075-8

Bryan SE, Tipping E, Hamilton-Taylor J (2002) Comparison of measured and modelled copper binding by natural organic matter in freshwaters. Comp Biochem Physiol - C Toxicol Pharmacol 133:37–49 . doi: 10.1016/S1532-0456(02)00083-2

Buffle J, Chalmers RA, Masson MR, Midgley MD (1988) Complexation Reactions in Aquatic Systems: An Analytical Approach. E. Horwood

Butman DE, Raymond PA, Butler KD, Aiken GR (2012) Relationships between δ14C and the molecular quality of dissolved organic carbon in rivers draining to the coast from the conterminous United States. Global Biogeochem Cycles 26:1–15 . doi: 10.1029/2012GB004361

Butman DE, Wilson HF, Barnes RT, et al (2015) Increased mobilization of aged carbon to rivers by human disturbance. Nat Geosci 8:112–116 . doi: 10.1038/ngeo2322

Chester R (1990) Marine Chemistry

Cory RM, McKnight DM (2005) Fluorescence Spectroscopy Reveals Ubiquitous Presence of Oxidized and Reduced Quinones in Dissolved Organic Matter. Environ Sci Technol 39:8142–8149

Cubasch U, Wuebbles D, Chen D, et al (2013) Introduction. In: Stocker TF, Qin D, Plattner G-K, et al. (eds) Climate Change 2013: The Physical Science Basis. Contribution of Working Group I to the Fifth Assessment of the Intergovernmental Panel on Climate Change.

Cambridge University Press, Cambridge, United Kingdom and New York, NY, USA
Dai M-H, Martin J (1995) First data on trace metal level and behaviour in two major Arctic river-estuarine systems (Ob and Yenisey) and in the adjacent Kara Sea, Russia. Earth Planet Sci Lett 131:127–141
de Baar HJW, de Jong JTM (2001) Distributions Sources and Sinks of Iron in Seawater. In: Turner DR, Hunter KA (eds) The Biogeochemistry of Iron in Seawater. John Wiley & Sons, Ltd., pp 124–253
Ekström SM, Regnell O, Reader HE, et al (2016) Increasing concentrations of iron in surface waters as a consequence of reducing conditions in the catchment area. JGR Biogeosciences 121:479–493 . doi: 10.1002/2015JG003141.Received
Fellman JB, Hood E, Edwards RT, Amore DVD (2009) Changes in the concentration, biodegradability, and fluorescent properties of dissolved organic matter during stormflows in coastal temperate watersheds. 114:1–14 . doi: 10.1029/2008JG000790
Francko DA, Heath RT (1982) UV-sensitive complex phosphorus: Association with dissolved humic material and iron in a bog lake1. Limnol Oceanogr 27:564–569 . doi: 10.4319/lo.1982.27.3.0564
Fujii M, Dang TC, Rose AL, et al (2011) Effect of Light on Iron Uptake by the Freshwater Cyanobacterium Microcystis aeruginosa. Environ Sci Technol 45:1391–1398 . doi: 10.1021/es103311h
Fujii M, Imaoka A, Yoshimura C, Waite TD (2014) Effects of molecular composition of natural organic matter on ferric iron complexation at circumneutral pH. Environ Sci Technol 48:4414–4424 . doi: 10.1021/es405496b
Gledhill M, van den Berg CMG (1994) Determination of complexation of iron(III) with natural organic complexing ligands in seawater using cathodic stripping voltammetry. Mar Chem 47:41–54 . doi: 10.1016/0304-4203(94)90012-4
Griffith DR, Raymond PA (2011) Multiple-source heterotrophy fueled by aged organic carbon in an urbanized estuary. Mar Chem 124:14–22 . doi: 10.1016/j.marchem.2010.11.003
Hassler CS, Havens SM, Bullerjahn GS, et al (2009) An evaluation of iron bioavailability and speciation in western Lake Superior with the use of combined physical, chemical, and biological assessment. Limnol Oceanogr 54:987–1001 . doi: 10.4319/lo.2009.54.3.0987
Hedges JI, Ertel JR, Quay PD, et al (1986) Organic Carbon-14 in the Amazon River System. Science (80-) 231:1112 . doi: 10.1126/science.231.4742.1129
Helms JR, Mao J, Schmidt-rohr K, et al (2013a) Photochemical flocculation of terrestrial dissolved organic matter and iron. Geochim Cosmochim Acta 121:398–413 . doi: 10.1016/j.gca.2013.07.025
Helms JR, Stubbins A, Perdue EM, et al (2013b) Photochemical bleaching of oceanic dissolved organic matter and its effect on absorption spectral slope and fluorescence. Mar Chem 155:81–91 . doi: 10.1016/j.marchem.2013.05.015
Helms JR, Stubbins A, Ritchie JD, et al (2008) Absorption spectral slopes and slope ratios as indicators of molecular weight, source, and photobleaching of chromophoric dissolved organic matter. Limnol Oceanogr 53:955–969 . doi: 10.4319/lo.2008.53.3.0955
Hernes PJ (2003) Photochemical and microbial degradation of dissolved lignin phenols: Implications for the fate of terrigenous dissolved organic matter in marine environments. J Geophys Res 108:3291 . doi: 10.1029/2002JC001421
Hernes PJ, Benner R (2003) Photochemical and microbial degradation of dissolved lignin phenols: Implications for the fate of terrigenous dissolved organic matter in marine environments. J

Geophys Res 108:3291 . doi: 10.1029/2002JC001421
Herzog SD, Persson P, Kvashnina K, Kritzberg ES (2020) Organic iron complexes enhance iron transport capacity along estuarine salinity gradients of Baltic estuaries. 331–344
Ho P, Joon M, Howden SD, Shiller AM (2019) Temporal and spatial distributions of nutrients and trace elements (Ba, Cs, Cr, Fe, Mn, Mo, U, V and Re) in Mississippi coastal waters: Influence of hypoxia, submarine groundwater discharge, and episodic events. Cont Shelf Res 175:53–69 . doi: 10.1016/j.csr.2019.01.013
Hood E, Gooseff MN, Johnson SL (2006) Changes in the character of stream water dissolved organic carbon during flushing in three small watersheds , Oregon. 111:1–8 . doi: 10.1029/2005JG000082
Hosen JD, Aho KS, Appling AP, et al (2019) Enhancement of primary production during drought in a temperate watershed is greater in larger rivers than headwater streams. Limnol Oceanogr 64:1458–1472 . doi: 10.1002/lno.11127
Hutchins DA, Bruland KW (1998) Iron-limited diatom growth and Si:N uptake ratios in a coastal upwelling regime. Lett to Nat 393:65–68
Imai A, Fukushima T, Matsushige K (1999) Effects of iron limitation and aquatic humic substances on the growth of Microcystis aeruginosa. Can J Fish Aquat Sci 56:1929–1937 . doi: 10.1139/cjfas-56-10-1929
Ingri J, Malinovsky D, Rodushkin I, et al (2006) Iron isotope fractionation in river colloidal matter. Earth Planet Sci Lett 245:792–798 . doi: 10.1016/j.epsl.2006.03.031
Jirsa F, Neubauer E, Kittinger R, et al (2013) Natural organic matter and iron export from the Tanner Moor, Austria. Limnologica 43:239–244 . doi: 10.1016/j.limno.2012.09.006
Joung D, Shiller AM (2016) Temporal and spatial variations of dissolved and colloidal trace elements in Louisiana Shelf waters. Mar Chem 181:25–43 . doi: 10.1016/j.marchem.2016.03.003
Kikuchi T, Fujii M, Terao K, et al (2017) Correlations between aromaticity of dissolved organic matter and trace metal concentrations in natural and effluent waters: A case study in the Sagami River Basin, Japan. Sci Total Environ 576:36–45 . doi: 10.1016/j.scitotenv.2016.10.068
Kinniburgh DG, van Riemsdijk WH, Koopal LK, et al (1999) Ion binding to natural organic matter: Competition, heterogeneity, stoichiometry and thermodynamic consistency. Colloids Surfaces A Physicochem Eng Asp 151:147–166 . doi: 10.1016/S0927-7757(98)00637-2
Koenings JP, Hooper FF (1976) The influence of colloidal organic matter on iron and iron-phosphorus cycling in an acid bog lake. Limnol Oceanogr 21:684–696 . doi: 10.4319/lo.1976.21.5.0674
Krachler R, Jirsa F, Ayromlou S (2005) Factors influencing the dissolved iron input by river water to the open ocean. Biogeosciences Discuss 2:537–549 . doi: 10.5194/bgd-2-537-2005
Krachler R, Krachler RF, Valda A, Keppler BK (2019) Natural iron fertilization of the coastal ocean by “blackwater rivers.” Sci Total Environ 656:952–958 . doi: 10.1016/j.scitotenv.2018.11.423
Krachler R, Krachler RF, von der Kammer F, et al (2010) Relevance of peat-draining rivers for the riverine input of dissolved iron into the ocean. Sci Total Environ 408:2402–2408 . doi: 10.1016/j.scitotenv.2010.02.018
Krachler R, Krachler RF, Wallner G, et al (2016) Sphagnum-dominated bog systems are highly effective yet variable sources of bio-available iron to marine waters. Sci Total Environ 556:53–62 . doi: 10.1016/j.scitotenv.2016.03.012

Kritzberg ES, Ekström SM (2012) Increasing iron concentrations in surface waters – a factor behind brownification? Biogeosciences 9:1465–1478 . doi: 10.5194/bg-9-1465-2012
Mayorga E, Aufdenkampe AK, Masiello CA, et al (2005) Young organic matter as a source of carbon dioxide outgassing from Amazonian rivers. Lett to Nat 436:538–541 . doi: 10.1038/nature03880
Medeiros PM, Seidel M, Gifford SM, et al (2017) Microbially-mediated transformations of estuarine dissolved organic matter. Front Mar Sci 4: . doi: 10.3389/fmars.2017.00069
Meybeck M (1982) Carbon, nitrogen, and phosphorous transport by world rivers. Science (80-) 282:401–450
Nagai T, Imai A, Matsushige K, et al (2004) Voltammetric determination of dissolved iron and its speciation in freshwater. Limnology 5:87–94 . doi: 10.1007/s10201-004-0121-x
Nagai T, Imai A, Matsushige K, Fukushima T (2006) Effect of iron complexation with dissolved organic matter on the growth of cyanobacteria in a eutrophic lake. Aquat Microb Ecol 44:231–239 . doi: 10.3354/ame044231
Neal C, Lofts S, Evans CD, et al (2008) Increasing iron concentrations in UK upland waters. Aquat Geochemistry 14:263–288 . doi: 10.1007/s10498-008-9036-1
Neubauer E, Köhler SJ, Von Der Kammer F, et al (2013) Effect of pH and stream order on iron and arsenic speciation in boreal catchments. Environ Sci Technol 47:7120–7128 . doi: 10.1021/es401193j
Norrström AC (1995) Concentration and chemical species of iron in soils from groundwater/surface water ecotones. Hydrol Sci 40:319–329 . doi: 10.1080/02626669509491418
O'Brien BJ (1986) The use of natural and anthropgenic 14C to investigate the dynamics of soil organic carbon. Radiocarbon 28:358–362
Parlanti E, Wörz K, Geoffroy L, Lamotte M (2000) Dissolved organic matter fluorescence spectroscopy as a tool to estimate biological activity in a coastal zone submitted to anthropogenic inputs. Org Geochem 31:1765–1781 . doi: 10.1016/S0146-6380(00)00124-8
Pokrovsky OS, Schott J (2002) Iron colloids/organic matter associated transport of major and trace elements in small boreal rivers and their estuaries (NW Russia). Chem Geol 190:141–179 . doi: 10.1016/S0009-2541(02)00115-8
Poulin BA, Ryan JN, Aiken GR (2014) Effects of Iron on Optical Properties of Dissolved Organic Matter. Environ Sci Technol 48:10098–10106 . doi: 10.1021/es502670r
Powell RT, Wilson-Finelli A (2003) Importance of organic Fe complexing ligands in the Mississippi River plume. Estuar Coast Shelf Sci 58:757–763 . doi: 10.1016/S0272-7714(03)00182-3
Qu B, Sillanpää M, Li C, et al (2017) Aged dissolved organic carbon exported from rivers of the Tibetan Plateau. PLoS One 12:1–11 . doi: 10.1371/journal.pone.0178166
Raymond PA, Bauer JE (2001a) Use of 14C and 13C natural abundances for evaluating riverine, estuarine, and coastal DOC and POC sources and cycling: A review and synthesis. Org Geochem 32:469–485 . doi: 10.1016/S0146-6380(00)00190-X
Raymond PA, Bauer JE (2001b) Riverine export of aged terrestrial organic matter to the North Atlantic Ocean. Nature 409:497–500 . doi: 10.1038/35054034
Raymond PA, Bauer JE, Caraco NF, et al (2004) Controls on the variability of organic matter and dissolved inorganic carbon ages in northeast US rivers. Mar Chem 92:353–366 . doi: 10.1016/j.marchem.2004.06.036
Raymond PA, McClelland JW, Holmes RM, et al (2007) Flux and age of dissolved organic carbon

exported to the Arctic Ocean: A carbon isotopic study of the five largest arctic rivers. Global Biogeochem Cycles 21:1–9 . doi: 10.1029/2007GB002934
Raymond PA, Saiers JE (2010) Event controlled DOC export from forested watersheds. Biogeochemistry 100:197–209 . doi: 10.1007/s10533-010-9416-7
Raymond PA, Saiers JE, Sobczak W V. (2016) Hydrological and biogeochemical controls on watershed dissolved organic matter transport: pulse-shunt concept. Ecology 97:5–16
Raymond PA, Spencer RGM (2015) Riverine DOM. In: Hansell DA, Carlson CA (eds) Biogeochemistry of Marine Dissolved Organic Matter, 2nd edn. Elsevier Inc., pp 509–533
Rijkenberg MJA, Gerringa LJA, Velzeboer I, et al (2006) Iron-binding ligands in Dutch estuaries are not affected by UV induced photochemical degradation. Mar Chem 100:11–23 . doi: 10.1016/j.marchem.2005.10.005
Rijkenberg MJA, Middag R, Laan P, et al (2014) The Distribution of Dissolved Iron in the West Atlantic Ocean. PLoS One 9:1–14 . doi: 10.1371/journal.pone.0101323
Rose AL, Waite TD (2003) Kinetics of iron complexation by dissolved natural organic matter in coastal waters. Mar Chem 84:85–103 . doi: 10.1016/S0304-4203(03)00113-0
Schlesinger WH, Bernhardt ES (2013) Biogeochemistry: An analysis of global change
Shapiro J (1977) On the measurement of ferrous iron in natural waters. Limnol Oceanogr 293–298
Shapiro J (1964) Effect of Yellow Organic Acids on Iron and Other Metals in Water. J Am Water Works Assoc 56:1062–1082
Shiller AM (1997) Dissolved trace elements in the Mississippi River: Seasonal, interannual, and decadal variability. Geochim Cosmochim Acta 61:4321–4330
Shiller AM (2003) Syringe Filtration Methods for Examining Dissolved and Colloidal Trace Element Distributions in Remote Field Locations. Environ Sci Technol 37:3953–3957 . doi: 10.1021/es0341182
Sholkovitz ER, Boyle EA, Price NB (1978) The removal of dissolved humic acids and iron during estuarine mixing. Earth Planet Sci Lett 40:130–136 . doi: 10.1016/0012-821X(78)90082-1
Shultz M, Pellerin B, Aiken GR, et al (2018) High Frequency Data Exposes Nonlinear Seasonal Controls on Dissolved Organic Matter in a Large Watershed. Environ Sci Technol 52:5644–5652
Stedmon CA, Markager S, Bro R (2003) Tracing dissolved organic matter in aquatic environments using a new approach to fluorescence spectroscopy. Mar Chem 82:239–254 . doi: 10.1016/S0304-4203(03)00072-0
Stefánsson A (2007) Iron (III) Hydrolysis and Solubility at 25 ° C. Environ Sci Technol 4:6117–6123 . doi: 10.1021/es070174h
Stolpe B, Guo L, Shiller AM, Aiken GR (2012) Abundance, size distributions and trace-element binding of organic and iron-rich nanocolloids in Alaskan rivers, as revealed by field-flow fractionation and ICP-MS. Geochim Cosmochim Acta 105:221–239 . doi: 10.1016/j.gca.2012.11.018
Stolpe B, Guo L, Shiller AM, Hassellöv M (2010) Size and composition of colloidal organic matter and trace elements in the Mississippi River, Pearl River and the northern Gulf of Mexico, as characterized by flow field-flow fractionation. Mar Chem 118:119–128 . doi: 10.1016/j.marchem.2009.11.007
Stolpe B, Hassellöv M, Andersson K, Turner DR (2005) High resolution ICPMS as an on-line detector for flow field-flow fractionation; multi-element determination of colloidal size distributions in a natural water sample. Anal Chim Acta 535:109–121 . doi: 10.1016/j.aca.2004.11.067

Striegl RG, Dornblaser MM, Aiken GR, et al (2007) Carbon export and cycling by the Yukon, Tanana, and Porcupine rivers, Alaska, 2001-2005. Water Resour Res 43:2001–2005 . doi: 10.1029/2006WR005201

Sunda WG, Huntsman SA (1995) Iron uptake and growth limitation in oceanic and coastal phytoplankton. Mar Chem 50:189–206

Tagliabue A, Aumont O, DeAth R, et al (2016) How well do global ocean biogeochemistry models simulate dissolved iron concentrations? Global Biogeochem Cycles 30:149–174 . doi: 10.1002/2015GB005289.Received

Tagliabue A, Bowie AR, Boyd PW, et al (2017) The integral role of iron in ocean biogeochemistry. Nature 543:51–59 . doi: 10.1038/nature21058

Theis TL, Singer PC (1974) Complexation of Iron(II) by Organic Matter and Its Effect on Iron(II) Oxygenation. Environ Sci Technol 8:569–573 . doi: 10.1021/es60091a008

Vieira LH, Krisch S, Hopwood MJ, et al (2020) Unprecedented Fe delivery from the Congo River margin to the South Atlantic Gyre. Nat Commun 11:1–8 . doi: 10.1038/s41467-019-14255-2

Vuori K-M (1995) Direct and indirect effects of iron on river ecosystems. Ann Zool Fenn 32:317–329

Wang W, Chen M, Guo L, Wang WX (2017) Size partitioning and mixing behavior of trace metals and dissolved organic matter in a South China estuary. Sci Total Environ 603–604:434–444 . doi: 10.1016/j.scitotenv.2017.06.121

Weishaar JL, Aiken GR, Bergamaschi BA, et al (2003) Evaluation of specific ultraviolet absorbance as an indicator of the chemical composition and reactivity of dissolved organic carbon. Environ Sci Technol 37:4702–4708 . doi: 10.1021/es030360x

Wershaw RL, Leenheer JA, Cox L (2005) Characterization of dissolved and particulate natural organic matter (NOM) in Neversink Reservoir, New York. US Geol Surv Sci Investig Rep

Wilson HF, Raymond PA, Saiers JE, et al (2016) Increases in humic and bioavailable dissolved organic matter in a forested New England headwater stream with increasing discharge. Mar Freshw Res 67:1279–1292 . doi: 10.1071/MF15286

Wilson HF, Xenopoulos MA (2008) Effects of agricultural land use on the composition of fluvial dissolved organic matter. Nat Geosci 2:37–41 . doi: 10.1038/ngeo391

Woods Hold Oceanographic Institute (2018) Radiocarbon Data & Calculations. https://www.whoi.edu/nosams/radiocarbon-data-calculations. Accessed 30 Jan 2020

Wu F, Evans D, Dillon P, Schiff S (2004) Molecular size distribution characteristics of the metal-DOM complexes in stream waters by high-performance size-exclusion chromatography (HPSEC) and high-resolution inductively coupled plasma mass spectrometry (ICP-MS). J Anal At Spectrom 19:979 . doi: 10.1039/b402819h

Xiao Y-H, Räike A, Hartikainen H, Vähätalo A V (2015) Iron as a source of color in river waters. Sci Total Environ 536:914–923 . doi: 10.1016/j.scitotenv.2015.06.092

Xiao Y-H, Sara-aho T, Va A V (2013) Contribution of ferric iron to light absorption by chromophoric dissolved organic matter. Limnol Oceanogr 58:653–662 . doi: 10.4319/lo.2013.58.2.0653

Xu H, Guan D, Zou L, et al (2018) Contrasting effects of photochemical and microbial degradation on Cu(II) binding with fluorescent DOM from different origins. Environ Pollut 239:205–214 . doi: 10.1016/j.envpol.2018.03.108

Yang R, Su H, Qu S, Wang X (2017) Capacity of humic substances to complex with iron at different salinities in the Yangtze River estuary and East China Sea. Sci Rep 1–9 . doi: 10.1038/s41598-017-01533-6

Yoon B, Raymond PA (2012) Dissolved organic matter export from a forested watershed during Hurricane Irene. Geophys Res Lett 39:1–6 . doi: 10.1029/2012GL052785